(p)ppGpp/GTP and malonyl-CoA modulate *Staphylococcus aureus* adaptation to FASII antibiotics and provide a basis for synergistic bi-therapy

Amit Pathania[1*], Jamila Anba-Mondoloni[1], Myriam Gominet[2], David Halpern[1], Julien Dairou[3], Laëtitia Dupont[1], Gilles Lamberet[1], Patrick Trieu-Cuot[2], Karine Gloux[1] and Alexandra Gruss[1*]

[1]Micalis Institute, INRAE, AgroParisTech, Université Paris-Saclay, Jouy en Josas, France, [2]Unité de Biologie des Pathogènes à Gram-positif, CNRS UMR 2001, Institut Pasteur, Paris, France, [3]Université Paris Descartes CNRS UMR 8601, Paris, France

* For correspondence:

amit.pathania@inrae.fr ORCID 0000-0003-2304-5060

alexandra.gruss@inrae.fr ORCID 0000-0001-7426-5229

Keywords: anti-FASII adaptation, (p)ppGpp, GTP, malonyl-CoA, phospholipids, antibiotic bi-therapy, triclosan, mupirocin, CodY

Running title: Metabolites set timing for anti-FASII adaptation

Abstract

Fatty acid biosynthesis (FASII) enzymes are considered valid targets for antimicrobial drug development against the human pathogen *Staphylococcus aureus*. However, incorporation of host fatty acids confers FASII antibiotic adaptation that compromises prospective treatments. *S. aureus* adapts to FASII inhibitors by a first non-replicative latency period followed by outgrowth. Here we used transcriptional fusions and direct metabolite measurements to investigate the factors that dictate the duration of latency prior to outgrowth. We show that stringent response induction leads to repression of FASII and phospholipid synthesis genes. (p)ppGpp induction inhibits synthesis of malonyl-CoA, a molecule that derepresses FapR, a key regulator of FASII and phospholipid synthesis. Anti-FASII treatment also triggers transient expression of (p)ppGpp-regulated genes during the anti-FASII latency phase, with concomitant repression of FapR regulon expression. These effects are reversed upon outgrowth. GTP depletion, a known consequence of stringent response, also occurs during FASII latency, and is proposed as the common signal linking these responses. We next show that anti-FASII treatment shifts malonyl-CoA distribution between its interactants FapR and FabD, towards FapR, increasing expression of phospholipid synthesis genes *plsX* and *plsC* during outgrowth. We conclude that components of the stringent response dictate malonyl-CoA availability in *S. aureus* FASII regulation, and contribute to latency prior to anti-FASII-adapted outgrowth. A combinatory approach, coupling a (p)ppGpp inducer and an anti-FASII, blocks *S. aureus* outgrowth, opening perspectives for bi-therapy treatment.

Importance

Staphylococcus aureus is a major human bacterial pathogen for which new inhibitors are urgently needed. Antibiotic development has centered on the fatty acid synthesis (FASII) pathway, which provides the building blocks for bacterial membrane phospholipids. However, *S. aureus* overcomes FASII inhibition and adapts to anti-FASII by using exogenous fatty acids that are abundant in host environments. This adaptation mechanism comprises a transient latency period, followed by bacterial outgrowth. Here we use metabolite sensors and promoter reporters to show that responses to stringent conditions and to FASII inhibition intersect: both involve GTP and malonyl-CoA. These two signaling molecules contribute to modulating the duration of latency prior to *S. aureus* adaptation outgrowth. We exploit these novel findings to propose a bi-therapy treatment against staphylococcal infections.

58 **Introduction**

59 Bacterial infections that fail to respond to antibiotic treatments are on the rise, especially in the
60 immunocompromised or weakened host, underlining the need for novel antimicrobial strategies
61 (1). The fatty acid synthesis (FASII) enzymes were considered as fail-safe targets for eliminating
62 numerous gram-positive pathogens. Anti-FASII has been a front-line drug against *Mycobacterium*
63 *tuberculosis*, which synthesize very long chain fatty acids that cannot be compensated by the
64 environment (2). However, Firmicute pathogens, including *Staphylococcus aureus* and numerous
65 streptococcaceae, bypass FASII inhibition and satisfy their fatty acid requirements by using host-
66 supplied fatty acids (3-5). FASII inhibitors like triclosan (Tric), MUT056399, fasamycins A and B,
67 amycomicin and a pipeline FASII antibiotic AFN-1252 (6-11), would thus have limited use as stand-
68 alone treatments of infections by numerous gram-positive pathogens (3-5).

69 Our recent studies show that *S. aureus* can adapt to FASII inhibitors by two mechanisms,
70 depending on growth conditions. One involves mutations in a FASII initiation gene, usually *fabD*.
71 Lower activity of the FabD mutant would increase availability of its substrates, one of which is acyl
72 carrier protein (ACP), for incorporation of exogenous fatty acids (eFA) *via* the phosphate
73 acyltransferase PlsX (**Fig. S1A**) (4, 12). The second mode of adaptation occurs without FASII
74 mutations and predominates in serum-supplemented medium. In this case, full adaptation and eFA
75 incorporation in actively growing cells is achieved after a latency phase, whose duration (6-12 h)
76 depends on the strain and pre-growth in serum-containing medium. Adaptation is associated with
77 greater intracellular retention of eFA and ACP, which both contribute to eFA incorporation in
78 membrane phospholipids to compensate FASII inhibition (**Fig. S1B** (5)).

79 The factors regulating *S. aureus* transition from latency to outgrowth upon anti-FASII
80 treatment remain unknown. We hypothesized that initial fatty acid starvation in response to anti-
81 FASII might comprise the signal that delays eFA incorporation in phospholipids and outgrowth. The
82 *S. aureus* FapR repressor reportedly regulates most FASII genes (except *acc*, encoding acetyl-CoA
83 carboxylase, and FabZ, β-hydroxyacyl-ACP dehydratase), and phospholipid synthesis genes *plsX* and
84 *plsC* (13, 14). Interestingly, malonyl-CoA has a dual function: it is the first dedicated FASII substrate
85 used by FabD (malonyl-CoA transacylase), and it also controls FapR by a feed-forward mechanism
86 (14). FabD uses malonyl-CoA and ACP to synthesize malonyl-ACP (15). Malonyl-CoA binding to FapR
87 reverses FapR repression, leading to up-regulation of the FASII and phospholipid synthesis genes
88 (14). Thus, malonyl-CoA is important in both enzymatic and regulatory activities of FASII. In

89 *Escherichia coli*, expression of the malonyl-CoA synthesis enzyme ACC is regulated by (p)ppGpp,
90 which accumulates in slow growing, nutrient-deficient conditions (16, 17); (p)ppGpp also reportedly
91 regulates other FASII and phospholipid synthesis genes (18, 19). In *B. subtilis*, studies of (p)ppGpp
92 null mutants gave evidence for the need to activate stringent response in order to survive fatty acid
93 starvation; these studies implicated increased GTP in mortality of (p)ppGpp null mutant strains (20).
94 Fatty acid starvation is also associated with cell size *via* regulation of FASII, although underlying
95 mechanisms remain to be elucidated (21). To our knowledge, no evidence exists for stringent
96 response-mediated FASII regulation in *S. aureus*.

97 Here, we first show that stringent response induction exerts control over fatty acid and
98 phospholipid synthesis in *S. aureus* by modulating FapR repressor activity. FASII antibiotic
99 treatment, like stringent response, leads to GTP depletion, which is the likely common metabolite
100 linking these two responses. The chain of events revealed here indicate that (p)ppGpp/GTP and
101 malonyl-CoA contribute to adjusting the timing of FASII-antibiotic-induced latency transition to
102 outgrowth. Based on our findings, we suggest a bi-therapy approach that combines FASII inhibitors
103 and a (p)ppGpp inducer to prevent *S. aureus* adaptation.

104

105 **Results**

106 **(p)ppGpp negatively regulates malonyl-CoA levels in *S. aureus*.**

107 We investigated the potential roles of (p)ppGpp and malonyl-CoA in *S. aureus* response to FASII
108 inhibition. Three *S. aureus* strains were used in this study, Newman, USA300, and HG1-R (**Table S1**),
109 which all adapt to anti-FASII with similar kinetics ((5), this study). Previous studies reported
110 difficulties in (p)ppGpp measurements in *B. subtilis* and *S. aureus* (20, 22). Our initial attempts at
111 measuring (p)ppGpp by HPLC and fluorescent dye PyDPA (23) failed to give reliable results (data not
112 shown). We therefore constructed transcriptional fusions to detect conditions when (p)ppGpp-
113 induced genes are activated *in vivo* (**Table S2**). The reporter fusion activities responded to
114 mupirocin, which inhibits isoleucyl-tRNA synthetase and triggers (p)ppGpp synthesis (24) (**Fig. 1A**
115 and data not shown). P_{ilvD}-*lacZ* (NWMN_1960) and P_{oppB}-*lacZ* (NWMN_0856) were up-regulated,
116 and P_{cshA}-*lacZ* (NWMN_1985) was down-regulated by mupirocin. Nutrient starvation during
117 stationary phase induces stringent response in *E. coli* (16). In *S. aureus*, β-galactosidase (β-gal)
118 activity of the P_{ilvD}-*lacZ* and P_{oppB}-*lacZ* sensors were 1.2- and 7- fold higher in stationary phase

119 compared to exponential phase cells, while P_{cshA}-*lacZ* activity was ~2-fold lower (**Fig. 1B** and data
120 not shown), further validating the *in vivo* (p)ppGpp sensors.

121 The stringent response sensors would expectedly not respond to mupirocin in a (p)ppGpp
122 null strain. We compared sensor responses in HG1-R and HG1R-ppGpp0 strains. These strains
123 derive from HG001 (25) and a (p)ppGpp-null strain (kindly provided by C. Wolz; (26)). They were
124 first repaired for a defect in *fakB1*, which is common to 8325 derivatives (like HG001) and a
125 minority of *S. aureus* isolates (5). FakB1, a fatty acid kinase subunit, facilitates assimilation of mainly
126 saturated fatty acids (27). Its absence in 8325 derivatives can explain previous reports of *S. aureus*
127 sensitivity to anti-FASII (11, 28), although the majority of *S. aureus* strains adapt to these antibiotics
128 (4, 5). The *fakB1*-repaired HG001 and HG001 (p)ppGpp0 strains are referred to as respectively HG1-
129 R and ppGpp0. Responses of the P_{ilvD}-*lacZ*, and P_{cshA}-*lacZ* reporter fusions were compared in HG1-R
130 and ppGpp0 strains by plate tests (**Figure S2; see Materials and Methods)**. If the response to
131 mupirocin occurs *via* its stimulation of (p)ppGpp, then neither induction of *ilvD* nor suppression of
132 *cshA* would occur in the ppGpp0 background. Indeed, P_{ilvD}-*lacZ* (**Fig. S2A**) and P_{cshA}-*lacZ* (**Fig. S2B**)
133 responded to mupirocin as expected in the parental strain, whereas no such responses were
134 observed in the ppGpp0 background. These results also indicate that stringent response controls
135 these sensors in *S. aureus*.

136 We then asked whether (p)ppGpp blocks malonyl-CoA synthesis in *S. aureus*, as reported in
137 *E. coli* (29), despite major regulatory differences between these bacteria**.** Total malonyl-CoA was
138 measured in cells treated or not with mupirocin by ELISA immunoassay. We also used *in vivo*
139 promoter fusion P_{accBC}-*lacZ* to measure expression of *accBC* (NWMN_1432 and NWMN_1431),
140 which encode subunits of acetyl-CoA carboxylase (ACC) required for malonyl-CoA synthesis (**Table**
141 **S2**). Stringent response induction by mupirocin led to decreases in malonyl-CoA pools (~6-fold) and
142 in P_{accBC}-*lacZ* β-gal activity (~4-fold) (**Fig. 1C**). Similarly, stationary phase cells showed ~2-fold lower
143 malonyl-CoA production and P_{accBC}-*lacZ* β-gal activity compared to exponential phase cells (**Fig. 1D**).
144 Finally, the P_{accBC}-*lacZ* reporter was inhibited by mupirocin in HG1-R, but not in the ppGpp0 strain
145 (**Fig. S2C**). These results show that in *S. aureus*, stringent response induction leads to repression of
146 malonyl-CoA synthesis (13).

147 **FASII-antibiotic-induced latency transiently alters expression of (p)ppGpp-regulated sensors.**

148 We recently showed that host fatty acids can compensate FASII-antibiotic inhibition of *S. aureus* to
149 promote growth. In low membrane stress conditions as in serum, adaptation involves a transient

150 latency phase without detection of FASII mutations (**Fig. 2A**). Anti-FASII-adapted *S. aureus* display
151 fatty acid profiles that are fully exogenous (**Fig. S1B**, (5)). As anti-FASII treatment may provoke fatty
152 acid deprivation before eFAs are incorporated, we asked whether the latency preceding FASII
153 bypass corresponds to stringent response induction. Using the stringent response sensors, a ~3.9-
154 fold increase in P_{ilvD}-*lacZ* and ~7-fold decrease of P_{cshA}-*lacZ* β-gal activities were observed during the
155 latency phase preceding outgrowth (**Fig. 2B**), indicating that a factor related to stringent response is
156 induced in response to anti-FASII treatment. P_{ilvD}-*lacZ* activity returned to normal levels once
157 bacteria are in the outgrowth phase. P_{cshA}-*lacZ* β-gal activity was only partially restored during
158 outgrowth, as levels increased by only 2-fold compared to latency. The reason for lower *cshA*
159 expression is unknown, but it is likely that its expression is subject to other layers of regulation.

160 **FASII antibiotic treatment down-regulates *accBC* and lowers malonyl-CoA pools.**

161 Malonyl-CoA, the ACC product, binds FapR and antagonizes repression, and is also a FabD substrate
162 (**Fig. 3A**). We assessed malonyl-CoA production in non-selective (SerFA) and anti-FASII-treated
163 (SerFA-Tric) latency and outgrowth Newman cultures. Pools of malonyl-CoA were measured by
164 ELISA and by P_{accBC}-*lacZ* expression. Both measurements indicated that malonyl-CoA levels were
165 comparable in SerFA and SerFA-Tric-adapted outgrowth cultures, and were markedly lower during
166 SerFA-Tric latency (**Fig. 3B**). Taken together these results show that stringent response induction
167 and anti-FASII-induced latency lead to *accBC* inhibition, suggesting that a common element links
168 these responses.

169 We also assessed pools of malonyl-CoA using a FapR activity sensor called FapR-Trap (**Fig.**
170 **S3A, Table S2**). FapR-Trap responded as expected: expression was increased in the absence of
171 repressor (Δ*fapR*), but decreased in stationary phase wild type cells when malonyl-CoA levels are
172 low (**Fig. S3B**). Interestingly, and in sharp contrast to the above results, malonyl-CoA estimations by
173 FapR-Trap were around 10-fold higher during SerFA-Tric outgrowth, compared to non-selective
174 SerFA cultures (**Fig. 3C**; compare with **3B**). These differences (summarized in **Table S3**), particularly
175 visible during adaptation outgrowth, indicate that malonyl-CoA distribution in anti-FASII-treated *S.*
176 *aureus* favors FapR binding over FabD. They suggest that malonyl-CoA pools and their distribution
177 between FapR and FabD may be central determinants in *S. aureus* adaptation to FASII antibiotics.

178 Reduced FabD competition for malonyl-CoA would increase its availability for FapR (**Fig. 3A**).
179 We showed previously that *fabD* mutants may emerge upon FASII-antibiotic selection, but not in

180 serum-supplemented medium as used here (4, 5). Indeed, a *fabD* mutant displayed 5-fold greater
181 FapR-Trap expression than the parental strain in non-selective SerFA (Fig. 3D). However, we ruled
182 out the presence of *fabD* mutations in our conditions by DNA sequencing of 5 independent anti-
183 FASII-adapted cultures (available upon request). These findings could suggest that FabD is intact,
184 but disabled for its interactions with malonyl-CoA during *S. aureus* growth in the presence of anti-
185 FASII. This possibility is currently under study in our laboratory.

186 **GTP depletion is the feature common to stringent response and FASII-antibiotic-induced latency.**

187 We asked whether stringent response effector (p)ppGpp was directly responsible for the observed
188 phenotypes during anti-FASII treatment, using a *S. aureus* WT (HG1-R) and the (p)ppGpp0 isogenic
189 strain. AFN-1252 was used as anti-FASII in this strain background due to higher resistance of HG001
190 derivatives to triclosan. The HG1-R and (p)ppGpp0 strains grew similarly in the presence of anti-
191 FASII, suggesting that the absence of (p)ppGpp did not accelerate anti-FASII adaptation (data not
192 shown). We then compared expression of P_{ilvD}-*lacZ* and P_{accBC}-*lacZ* sensors in the WT *versus*
193 (p)ppGpp0 backgrounds upon anti-FASII treatment (**Fig 4A**). Both sensors behaved as above (**Figs 2**
194 **and 3**) in the WT strain. However, these sensors displayed the same responses to anti-FASII
195 treatment in the two strains. Thus, while (p)ppGpp induction inhibits *acc* and thus lowers malonyl-
196 CoA pools, it is not required for these phenotypes in anti-FASII-treated *S. aureus*.

197 (p)ppGpp is known to be intimately linked to GTP: (p)ppGpp inhibits GTP synthesis (30, 31).
198 Lowering GTP rescues *B. subtilis* from ppGpp0 toxicity during lipid starvation(20). We used HPLC to
199 measure GTP levels during anti-FASII adaptation of *S. aureus* Newman. GTP levels decreased by 4-
200 fold at 3h post-anti-FASII treatment (**Fig. 4B**). Consistently, amounts of two GTP synthesis enzymes
201 were decreased during anti-FASII latency of *S. aureus* USA300, as seen by proteomics (5); HprT
202 (2.35-fold lower [n=4]; p=0.014) and GuaA (1.5-fold lower [n=4]; p=0.029). These results identify
203 GTP as the metabolite and potential effector common to both stringent response and anti-FASII-
204 induced latency.

205 GTP is also a cofactor of the pleiotropic regulator CodY (31). We asked whether CodY is
206 implicated in *accBC* regulation. P_{accBC}-*lacZ* expression was visibly lower in a *codY* insertional mutant
207 compared to expression in the parental WT (USA300) **(Fig. 4C).** In addition, the anti-FASII latency
208 period was strikingly longer in a *codY* mutant than in the WT strain (**Fig. 4D**). This delay is consistent
209 with a role of GTP depletion in delaying anti-FASII latency *via* CodY. These results lead us to propose

210 that in *S. aureus*, the stringent response pathway intersects the initial latency response to FASII
211 inhibitors by the common depletion of GTP, likely *via* the CodY regulon.

212 **Phospholipid synthesis genes *plsX* and *plsC* are differently controlled by FapR.**

213 The above results show that malonyl-CoA pools are restored during *S. aureus* adaptation to FASII
214 antibiotics, and preferentially bind FapR, which alleviates FapR repression **(Fig. 3)**. The *S. aureus*
215 FapR regulon reportedly includes *plsX* (NWMN_1139, part of the *fapR* operon) and *plsC*
216 (NWMN_1620); however, the *S. aureus* FapR binding site in the *plsC* promoter region is highly
217 degenerate ((13); see **Fig. 5A**), and no proof was given for this interaction. We used promoter
218 reporter fusions $P_{fapR\ plsX}$-*lacZ* and P_{plsC}-*lacZ* (**Table S2**) to compare expression in a wild type strain
219 (HG1-R) and its Δ*fapR* derivative. Expression of both reporters was upregulated (each 1.6-fold) in
220 the Δ*fapR* strain (**Fig. 5B**). To determine whether regulation involved direct FapR binding, we
221 performed DNase I footprinting using the *plsX* and *plsC* promoters as binding substrates for purified
222 FapR (**Fig. 5C**). FapR bound efficiently to the *plsX* promoter region. In contrast, FapR did not bind
223 the *plsC* upstream region containing the putative binding site. Taken together, these results
224 indicate that in *S. aureus*, FapR regulates expression of both *plsX* and *plsC*, but that its effect on *plsC*
225 is either indirect or may require other *S. aureus* factors.

226 **Mupirocin and anti-FASII treatment lead to reduced expression of *S. aureus* phospholipid**
227 **synthesis genes *plsX* and *plsC*.**

228 Repression of *accBC* FASII by mupirocin would expectedly impact all FapR-regulated genes,
229 including those involved in phospholipid synthesis (**Fig. S1A**). To test this, we followed $P_{fapRplsX}$-*lacZ*
230 and P_{plsC}-*lacZ* transcriptional fusion expression in the presence of mupirocin (0.1 µg/ml), using P_{ilvD}-
231 *lacZ* and P_{accBC}-*lacZ* sensors as references (**Table S4**). Expression of *plsX* and *plsC* sensor fusions
232 were 4- and 3-fold respectively lower in mupirocin than in non-treated samples.

233 Responses of $P_{fapRplsX}$-*lacZ* and P_{plsC}-*lacZ* during anti-FASII-induced latency and outgrowth
234 were then measured. β-gal expression from both sensors gradually decreased during latency,
235 followed by abrupt (respectively 4- and 2-fold) increases upon restart of active growth of anti-FASII
236 -adapted cells (**Fig. 5D**, and data not shown). Expression of $P_{fapRplsX}$-*lacZ* reached higher (~3-fold)
237 levels in anti-FASII-adapted outgrowth than in non-selective growth. Anti-FASII treatment thus
238 decreases expression of phospholipid synthesis genes during latency, which recovers upon
239 adaptation.

240

241

242 **Mupirocin treatment lowers fatty acid incorporation and is synergistic with anti-FASII to inhibit *S.***
243 ***aureus* growth.**

244 Since mupirocin leads to down-regulation of phospholipid synthesis genes, it might consequently
245 affect *S. aureus* membrane fatty acid composition. To test this, *S. aureus* Newman was grown in
246 SerFA without and with sublethal mupirocin addition (0.05 µg/ml, *i.e.*, 5-fold below the MIC; (32)).
247 Incorporated eFA was markedly decreased, from 50% in non-treated, to 35% in mupirocin cultures
248 (**Fig. 6A**). (p)ppGpp induction during anti-FASII-induced latency could thus slow or stop eFA
249 incorporation in this transient period.

250 The above findings led us to hypothesize that FASII inhibitors could be synergistic with a
251 stringent response inducer that prevents compensatory eFA incorporation by repressing
252 phospholipid synthesis genes *plsX* and *plsC*. We first examined anti-FASII adaptation in a strain
253 expressing (p)ppGpp (*via relP*-expressing plasmid pCG258 in a ppGpp0 strain; (26), **Table S2**). While
254 the ppGpp0 control strain (carrying the empty vector pCG248) adapted to anti-FASII after overnight
255 growth, basal RelP expression was sufficient to inhibit anti-FASII adaptation (**Fig. 6B**). This result
256 shows that (p)ppGpp accumulation synergizes with anti-FASII to block *S. aureus* growth. Likewise,
257 addition of a subinhibitory concentration of mupirocin (0.05 µg/ml) and triclosan (0.5 µg/ml) to *S.*
258 *aureus* SerFA cultures resulted in extended latency, whereas neither mupirocin nor the anti-FASII
259 separately blocked bacterial growth (**Fig. 6C**). Similar results were obtained using anti-FASII AFN-
260 1252 (7) and MRSA strain USA300 FPR3757 (**Table S5**). The observed synergistic effect between two
261 flawed antibiotics may offer an effective strategy for development of last-resort treatments against
262 *S. aureus* infection.

263

264 **Discussion**

265 This study reveals the nature of cross-control between *S. aureus* responses to FASII inhibition and
266 to stringent conditions. GTP is depleted in both these conditions, which may explain why the same
267 targets are affected. Our results further show that (p)ppGpp induction lengthens the latency phase
268 preceding adaptation to FASII inhibition. *accBC* transcription is repressed upon stringent response
269 induction, which sets off a chain of events leading to transient repression of phospholipid synthesis

270 genes *plsX* and *plsC*. These events correlate with limited eFA incorporation and extended latency.
271 During *S. aureus* adaptation outgrowth, the initial effects of anti-FASII are reversed, allowing eFA
272 incorporation and adaptation to FASII antibiotics. These results suggest a model (**Fig. 7**) in which
273 (p)ppGpp induction and anti-FASII both initially trigger GTP depletion, resulting in decreased
274 malonyl-CoA pools. The suggested role for CodY in regulating ACC expression remains to be
275 investigated. These events repress phospholipid enzyme synthesis and contribute to anti-FASII
276 latency prior to adaptation outgrowth. Stringent conditions in host niches may be relevant to *S.*
277 *aureus* infection (33), and might impact the bacterial response to anti-FASII treatment. While our
278 findings identify a role for (p)ppGpp induction *via* GTP depletion in anti-FASII adaptation in *S.*
279 *aureus*, they do not rule out other roles for these metabolites, or the involvement of other factors
280 in this process.

281 A new role for malonyl-CoA in anti-FASII adaptation is uncovered, *via* its increased
282 association with FapR in antibiotic-adapted cultures compared to non-selective cultures. FapR-Trap
283 showed ~10-fold greater expression in anti-FASII-adapted cultures than in non-selective cultures,
284 while total malonyl-CoA pools were the same in both conditions (**Fig. 3**). Increased malonyl-CoA
285 interaction with FapR, *i.e.*, FapR derepression, during anti-FASII adaptation is consistent with
286 increased *plsX* and *plsC* expression (**Fig. 5)**. Malonyl-CoA rerouting in anti-FASII may be explained by
287 FabD inactivation in anti-FASII adaptation conditions, e.g., by an intermediate metabolite as
288 suggested in *E. coli* (34). Along this line, a recent study proposed that acyl-ACP accumulation could
289 inhibit FabD (35). Interestingly, acyl-ACP accumulates in a *fabD* mutant during anti-FASII adaptation
290 (4). Alternative possibilities may be considered, such as i- post-translational FabD modification (36)
291 or ii- FabD reversal upon FASII inhibition due to a pile-up of its end-product, malonyl-ACP. We are
292 currently investigating these hypotheses. These findings indicate limits to the reliability of FapR
293 operon-based sensors to estimate malonyl-CoA pools, for which readouts vary according to growth
294 conditions. This may be important to consider in bioengineering applications that rely on FapR
295 operon-like sensors to optimize malonyl-CoA production (37)**.**

296 Previous studies identified *S. aureus plsC* as comprising a FapR binding site (13). This is
297 disproven here, as FapR failed to bind the published *plsC* consensus site, which lacks a consensus
298 palindromic sequence (**Fig. 5C**). Nevertheless, *plsC* expression is increased in a Δ*fapR* mutant,
299 indicating indirect FapR control of expression.

300 The need for antimicrobial alternatives is urgent and, besides the discovery of new
301 molecules or targets, the development of efficient combinations based on existing but individually
302 ineffective drugs remains to be explored. Our clarification of the link between stringent response
303 and anti-FASII adaptation opens perspectives for combinatorial antibiotic strategies, using FASII
304 inhibitor and subinhibitory concentrations of stringent response inducers that delay or prevent
305 anti-FASII adaptation of multidrug resistant pathogens like *S. aureus*. Mupirocin, which is usually
306 used topically, was recently proposed as a potentially active systemic antibiotic when presented in
307 liposomes (38). The proof of concept demonstrated here using anti-FASII antibiotics and mupirocin,
308 suggests a useful bi-therapy approach for reducing *S. aureus* survival during infection.

309

310

311

312 **Materials and Methods**

313 **Strains and media**

314 Strains are listed in **Table S1**. BHI (Brain Heart Infusion) and LB (Luria-Bertani) media were used
315 respectively for *S. aureus* and *E. coli* growth. *S. aureus* precultures were routinely prepared in BHI
316 medium. Three fatty acids (C14:0; myristic acid, C16:0; palmitic acid and C18:1; oleic acid;, Larodan
317 Fine Chemicals, Sweden) were prepared as 100 mM stocks in DMSO and used at final equimolar
318 concentrations of 0.17 mM each in experiments (referred as eFA). Ser-FA (BHI containing eFA+10%
319 newborn calf serum; Sigma) and SerFA-Tric (SerFA+Triclosan 0.5 µg/ml), or SerFA-AFN (SerFA+AFN-
320 1252 0.5 µg/ml) were the modified media used as indicated. Antibiotics kanamycin (50 µg/ml) and
321 erythromycin (5 µg/ml) were used in *E. coli* and *S. aureus* respectively to select pTCV-*lac*-based
322 reporter fusion plasmids (39). Antibiotic adaptation experiments with plasmid-carrying strains were
323 done in SerFA-Tric containing 2 µg/ml erythromycin; note that the latency period was extended by
324 about 4-6 h in this condition. Mupirocin (Sigma), a functional analogue of isoleucyl-AMP and a
325 stringent response inducer of (p)ppGpp (40) was prepared in DMSO and used at 0.1 µg/ml (32, 41)
326 to validate (p)ppGpp sensors, or at 0.05 µg/ml when used in combination with anti-FASII. Equal
327 volumes of DMSO were added to control samples when mupirocin was used.

328 **Growth experiments in anti-FASII**

329 Three *S. aureus* strains or their derivatives were used to follow anti-FASII adaptation: Newman,
330 USA300, and HG1-R. The latter strain corresponds to HG001 that was repaired for a *fakB1* defect
331 present in the 8325 lineage, and in a minority of *S. aureus* strains; *fakB1* encodes a fatty acid kinase
332 subunit for saturated fatty acid phosphorylation, which enables the use of eFA during anti-FASII
333 adaptation. The above strains showed comparable responses to conditions tested in this work. In
334 experiments using triclosan as anti-FASII, cells were precultured in BHI and then diluted to A_{600} =
335 0.01 in SerFA-Tric. Growth was followed by A_{600} readings as indicated. Nonselective exponential and
336 stationary phase cultures were harvested at A_{600}= 1-4, and ~10, respectively. If AFN-1252 was used
337 as anti-FASII, the procedure was the same except that pre-cultures were done in SerFA. Both
338 triclosan and AFN-1252 specifically inhibit FabI, a FASII enzyme (7, 42). Triclosan causes non-specific
339 membrane damage at higher concentrations (42), and was therefore not used in studies with the
340 HG1-R strain, which showed higher resistance to this drug.

341 **Construction of *fakB1*-repaired strains**

342 The *fakB1* gene of *S. aureus* HG001, as the entire 8325 lineage, displays a 483-bp deletion removing
343 56% of the 867-bp functional gene. To repair this deletion, a 1,939-bp DNA containing a functional
344 *fakB1* was amplified by PCR from *S. aureus* JE2 with primers fakB1_fp and fakB1_rp (**Table S6**). This
345 fragment was cloned using Gibson Assembly protocol in the thermosensitive vector pG1 (43)
346 amplified with the primers pG1_GibBam and pG1_GibEco (**Table S6**). The resulting vector
347 pG1Ω*fakB1* was introduced by electroporation in *S. aureus* HG001, HG001Δ*fapR*, and
348 HG001ppGpp0, to generate corresponding *fakB1*-repaired strains (**Table S1**). Electroporation of *S.*
349 *aureus* strains and allelic exchange were performed as described (44). The expected *fakB1*
350 reparation in these strains was confirmed by PCR and sequence analysis.

351 **Reporter fusions**

352 Promoter regions of *ilvD*, *oppB*, *cshA*, as well as *fapR*, *plsC* and *accBC*, were cloned in pTCV-*lac* or
353 pAW8 plasmids (**Table S2**) using the appropriate primers (**Table S6**). PCR-amplified DNA fragments
354 and plasmid were treated with restriction enzymes EcoRI and BamH1 and ligated products were
355 transformed into DH5α, Top10, or IM08B. The obtained constructs were confirmed by DNA
356 sequencing. Plasmids obtained from IM08B were used directly to transform the *S. aureus* Newman
357 strain; clones obtained in DH5α or Top10 were first established in RN4220. A standard
358 electroporation protocol was used to transform DNA in *S. aureus* (45).

359 **(p)ppGpp sensors**

360 *ilvD* (NWMN_1960) and *oppB* (NWMN_0856) are up-regulated, and *cshA* (NWMN_1985) genes is
361 down- regulated upon stringent response induction (24, 40, 46). The corresponding stringent
362 response sensors P_{ilvD}-*lacZ*, P_{oppB}-*lacZ*, and P_{cshA}-*lacZ* (**Table S2**) were tested in medium containing
363 0.1 µg/ml mupirocin (40), and validated as *bone fide* (p)ppGpp sensors (Fig. 1A).

364 **FapR activity sensor**

365 To estimate malonyl-CoA pools bound to FapR, we designed a transcriptional fusion with promoter
366 and operator sequences containing a consensus FapR binding site; FapR-Trap (**Fig. S2, Table S2**).
367 The construction was based on similar studies done previously to estimate malonyl-CoA pools (37,
368 47).

369 **β-galactosidase (β-gal) assay**

370 Fresh cultures were prepared at A_{600} = 0.1 from overnight BHI cultures and β-gal activities were
371 measured at the indicated A_{600} or time of sampling. When mupirocin was used, cultures were
372 treated or not at A_{600} = 0.1 after growth from an initial A_{600} = 0.01 and processed 1 h later. All
373 samples of a set were stored at -20°C prior to measurements, which were performed for all
374 samples of a same set. β-gal activities were measured as described (48), except that samples
375 derived from SerFA-containing medium were incubated with lysostaphin (0.1 mg/ml) for 30 min at
376 room temperature prior to processing with β-Glo™ reagents (Promega). β-gal values (mean ±
377 standard deviation) were determined from three independently performed experiments.

378 **Malonyl-CoA measurement by ELISA assay**

379 Bacterial cultures were prepared as above, and samples were processed at the indicated A_{600}/time
380 interval according to our test conditions. For each sample, the equivalent of A_{600} = 30 was
381 centrifuged at 8,000 rpm at room temperature for 5 min. Pelleted cells were immediately frozen in
382 liquid nitrogen and transferred to -80°C overnight. Ice cold PBS (Phosphate Buffer Saline) was used
383 to resuspend cells at 4°C, which were then sonicated in FastPrep (MP Biomedicals). Supernatants
384 were collected by centrifuging the cell slurry at 13,000 rpm at 4°C for 5 min, and stored at -80°C
385 until use. ELISA tests for total malonyl-CoA measurements were performed as per manufacturer's
386 instructions (CUSABIO). Malonyl-CoA standards were run along with test samples. Each experiment
387 was performed on three independent cultures. Mean values ± standard deviation are presented.

388 For malonyl-CoA measurements under stringent response conditions (Fig. 1C, left panel),
389 Newman was first grown in BHI to A_{600} of 0.5 from an initial inoculum of 0.01. Cultures were treated
390 or not with 0.1 µg/ml mupirocin for 30 minutes (A_{600} = ~1 for both samples). ELISA assays were
391 performed as above.

392 **Purification of *S. aureus* FapR**

393 The *S. aureus fapR* gene was amplified by PCR with FapRORFfp and FapRORFrp primers (**Table S6**)
394 and cloned into pET-21b to produce a recombinant FapR carrying an N-terminal His tag and TEV site
395 expressed in *E. coli* BL21/pDIA17 (13, 49). Bacterial cultures were grown at 37°C in LB containing
396 ampicillin (100 µg/ml) and chloramphenicol (10 µg/ml) until A_{600} = 0.6; expression was then
397 performed following addition of IPTG (0.5 mM) at 20°C for 17 hours. Bacteria were harvested by
398 centrifugation (5g wet weight), washed twice in PBS, and resuspended in 30 ml buffer A (50 mM
399 Tris-HCl pH 7,5, 300 mM NaCl, 1 mM DTT), Benzonase® Nuclease (Sigma-Aldrich) and a protease
400 inhibitor cocktail (Roche). Bacteria were lysed by passage through a CF Cell-Disrupter (Constant
401 Systems Ltd) at 4°C. The lysed culture was centrifuged at 46,000 x g for 1 hour and the supernatant
402 was loaded onto a 1-ml Protino® Ni-NTA column (Macherey-Nagel). The protein was eluted with
403 buffer A + 300 mM imidazole and protein-containing fractions were pooled and dialyzed overnight
404 in buffer A with TEV protease (1/10 w/w ratio) at 4°C (produced by the Pasteur Institute Production
405 and Purification of Recombinant Proteins Technological Platform). The His-Tag free protein was
406 loaded onto a 1-ml Ni-NTA column and collected. FapR was further purified using a HiLoad 16/60
407 Superdex 75 prep grade column (GE Healthcare) equilibrated with 20 mM Tris pH 7.5, 50 mM NaCl.
408 The purified protein was concentrated and stored at -80°C.

409 **DNase I footprinting**

410 $P_{fapRplsX}$ and P_{plsC} promoter probes were amplified by PCR from pJJ013 ($P_{fapR\ plsX}$-*lacZ*) and pJJ019
411 (P_{plsC}-*lacZ*) (**Table S2**), respectively, with specific promoter primers (P*fapRplsX*_Fw; P*plsC*_fd) and
412 vector primer (pTCV-*lac*_rev).

413 The 5' end of pTCV-*lac*_Rev was labeled with (γ-^{32}P)ATP, with T4 polynucleotide kinase.
414 Before the DNA binding reaction, purified FapR was dialyzed in 100 mM Na2HPO4/NaH2PO4 (pH 8),
415 250 mM NaCl, 10 mM MgCl2, DTT 5 mM, and 50% glycerol. DNase I footprinting reactions were
416 performed as described (50). Briefly, 0 to 12 nmol FapR was mixed with 0.2 pmol of DNA and
417 incubated with DNase 1 at room temperature (~24°C) for 1 min. Samples were analyzed by

418 electrophoresis on a 6% polyacrylamide gel containing 7 M urea. Maxam and Gilbert sequencing
419 ladders (G+A) were loaded on the same gel.

420 **Determination of *S. aureus* fatty acid profiles**

421 Fatty acid profiles were done as described (4). Newman pre-cultures prepared from two
422 independent colonies were diluted to A_{600} = 0.1 in SerFA and grown 3 h with and without mupirocin
423 (0.05 µg/ml). A_{600} of SerFA samples were ~2.5 and treated samples ~1.0**.** Percentage of eFA are
424 shown (mean ± standard deviation).

425 **GTP determinations**

426 All extraction steps were performed on ice. Cellular pellets were deproteinized with an equal
427 volume of 6% perchloric acid (PCA), vortex-mixed for 20 s, ice-bathed for 10 min, and vortex-mixed
428 again for 20 s. Acid cell extracts were centrifuged at 13,000 rpm for 10 min at 4°C. The resulting
429 supernatants were supplemented with an equal volume of bi-distilled water, vortex-mixed for 60 s,
430 and neutralized by addition of 2 M Na_2CO_3. Extracts were injected onto a C18 Supelco 5 µm (250 ×
431 4.6 mm) column (Sigma) at 45°C. The mobile phase was delivered at a flow-rate of 1 ml/min using
432 the following stepwise gradient elution program: A–B (60:40) at 0 min→(40:60) at 30 min→(40:60)
433 at 60 min. Buffer A contained 10 mM tetrabutylammonium hydroxide, 10 mM KH2PO4 and 0.25%
434 MeOH, and was adjusted to pH 6.9 with 1 M HCl. Buffer B consisted of 5.6 mM
435 tetrabutylammonium hydroxide, 50 mM KH2PO4 and 30% MeOH, and was neutralized to pH 7.0
436 with 1 M NaOH. Detection was done with a diode array detector (PDA). The LC Solution workstation
437 chromatography manager was used to pilot the HPLC instrument and to process the data. Products
438 were monitored spectrophotometrically at 254 nm, and quantified by integration of the peak
439 absorbance area, employing a calibration curve established with various known nucleosides. Finally,
440 a correction coefficient was applied to correct raw data for minor differences in the total number of
441 cells (by A_{600} measurements) determined in each culture condition.

442 **Statistical analyses**

443 Graphs and statistical analyses were prepared using GraphPad Prism Software. Mean and standard
444 deviation are presented for sensor fusions, ELISA readouts, fatty acid profile comparisons, and GTP
445 measurements. Statistical significance was determined by unpaired, non-parametric Mann Whitney
446 tests, as recommended for small sample sizes, here biological triplicates, and by a non-parametric,
447 unpaired Kruskal Wallis test for three-way comparisons.

448

449

450

451 **Acknowledgements**

452 We acknowledge the valuable comments of anonymous reviewers. We are thankful to Jong-In
453 Hong, Seoul National University, Korea, for the generous gift of PyDPA used in initial studies. C.
454 Thomas and members of the Institut Pasteur Production and Purification of Recombinant Proteins
455 Platform are gratefully acknowledged for providing purified FapR. Our colleagues P. Bouloc (I2BC,
456 France), C. Morvan (U. Paris-Descartes, France), and MicrobAdapt team members E. Borezée-
457 Durant, D. Lechardeur, G. Kénanian, R. Boudjemaa, and P. Gaudu gave valuable advice. G. Dubey
458 and N. Descoeudres provided kind support. We acknowledge financial support from DIM-MalInf (AP
459 fellowship), French Agence Nationale de la Recherche (StaphEscape project ANR-13001038) and
460 Fondation pour la Recherche Medicale (DBF20161136769). This work is dedicated to our friend and
461 colleague G. Lamberet, who passed away Dec 23, 2019.

462

463 **Author Contributions**

464 Physiology, molecular biology, (p)ppGpp, GTP, and malonyl-CoA estimation: AP, MG, LD, JD, DH,
465 PTC. Fatty Acid analyses: GL, KG and AG. Data analyses: AP, JAM, PTC, and AG. Statistical analysis:
466 DH. Experimental design and project conception: AP, PTC, AG. AG directed the project and AP, KG
467 and AG wrote the manuscript.

468

469 **Declaration of Interests**

470 The authors declare no competing interests.

471

472 **Figure legends**

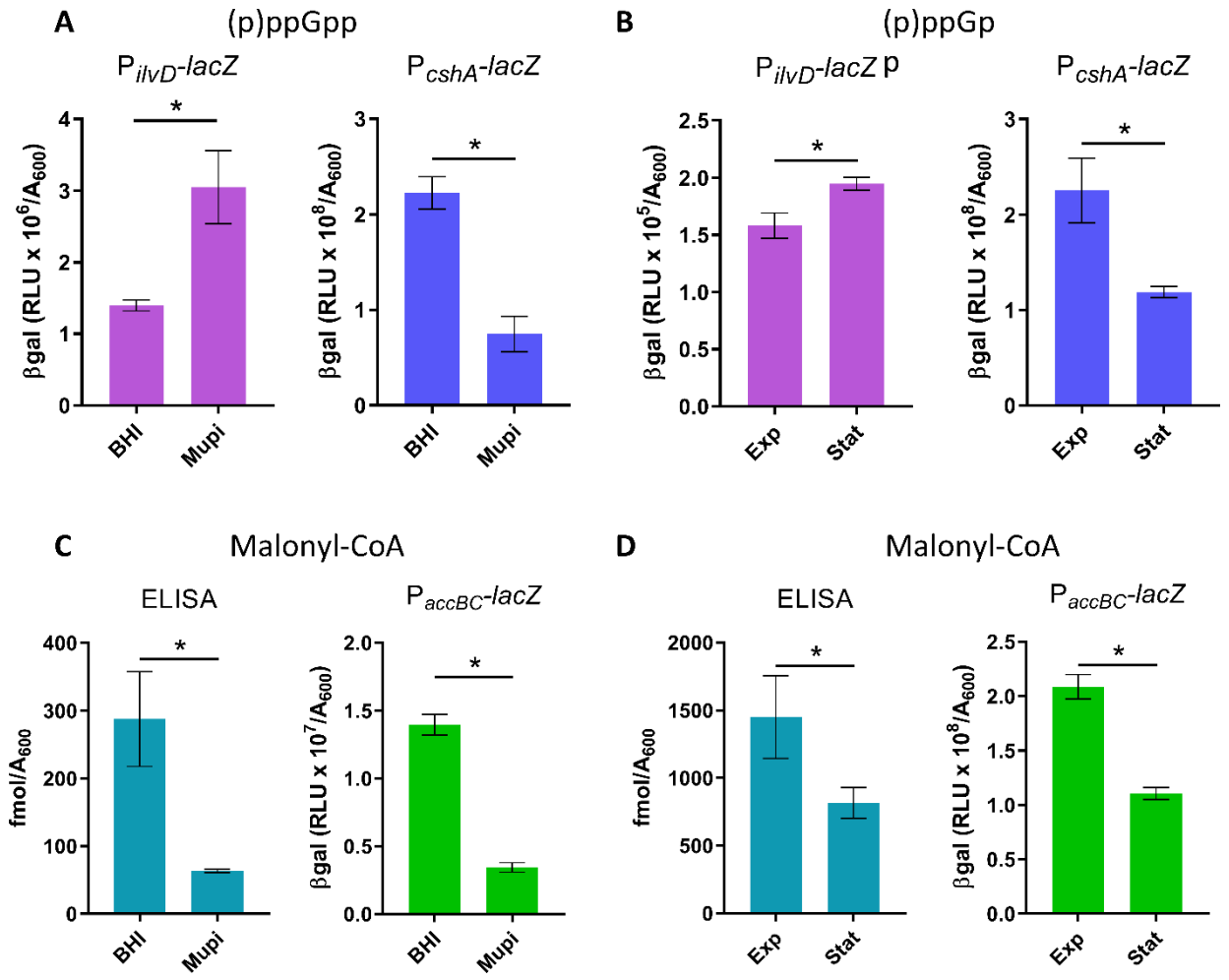

473

474 **Fig. 1. Mupirocin and stationary phase conditions stimulate (p)ppGpp sensor responses and**
475 **inhibit malonyl-CoA production and *accBC* activity.** *S. aureus* Newman strains contain reporter
476 systems as indicated. Strains were grown in BHI and BHI containing 0.1 µg/ml mupirocin (Mupi) for
477 1h (**A**,**C**), or in SerFA (A_{600} ~4.0, Exp) and stationary phase (A_{600} ~10.0, Stat) (**B** and **D**). P_{ilvD}-*lacZ* and
478 P_{cshA}-*lacZ* expression were evaluated by β-gal assays. Total Malonyl-CoA levels were determined by
479 immunoassay (ELISA), and deduced from P_{accBC}-*lacZ* expression. *ilvD* and *cshA* genes are respectively
480 up-regulated and down-regulated by stringent response induction. Data presented are mean ±
481 standard deviation from triplicate independent experiments. *, $p \leq 0.05$ using Mann Whitney.

482

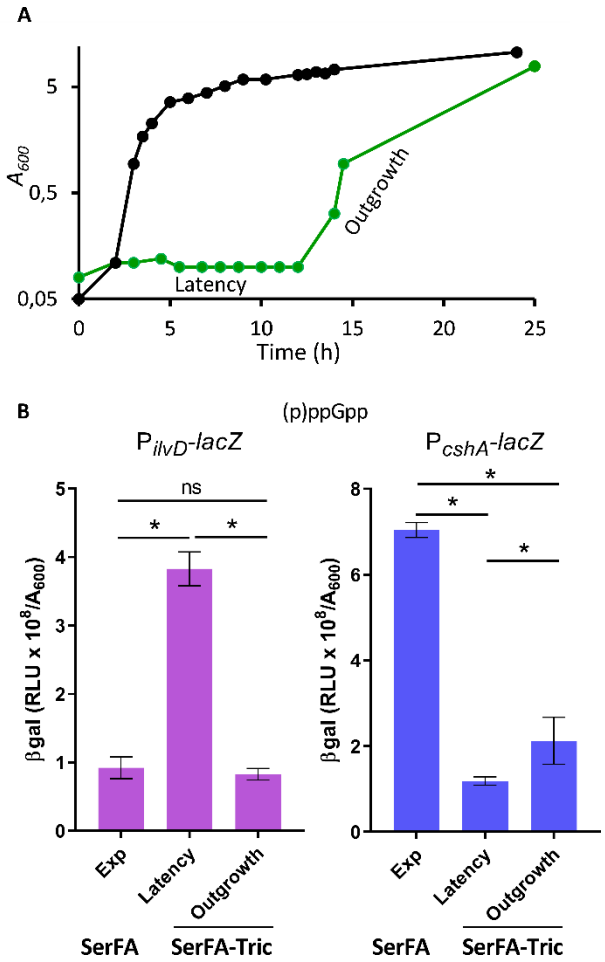

483

484 **Fig. 2. Anti-FASII treatment leads to transient responses of (p)ppGpp sensors. A.** Growth kinetics
485 of *S. aureus* Newman in SerFA (black line) and in SerFA-Tric (green). In SerFA-Tric, a 10-12 h latency
486 period (Latency) precedes exponential outgrowth (Outgrowth). The growth curves are
487 representative of three independent experiments. BHI and SerFA growth curves are essentially
488 identical; no growth is observed in BHI medium containing triclosan without fatty acids (n=3, not
489 shown). **B.** Stringent response status according to growth condition in Newman carrying P_{ilvD}-*lacZ*
490 reporter (left panel) and P_{cshA}-*lacZ* (right panel). β-gal activities of samples in SerFA (exponential
491 growth; Exp, A_{600} = ~1.5) and SerFA-Tric (Latency, A_{600} = ~0.3) are measured after 3 h growth. β-gal
492 activities were measured on 17 h samples in SerFA-Tric (exponential growth; Outgrowth, A_{600} =
493 ~1.5). Data presented are mean ± standard deviation from triplicate independent experiments. *, p
494 ≤ 0.05, ns, not significant, using Mann Whitney.

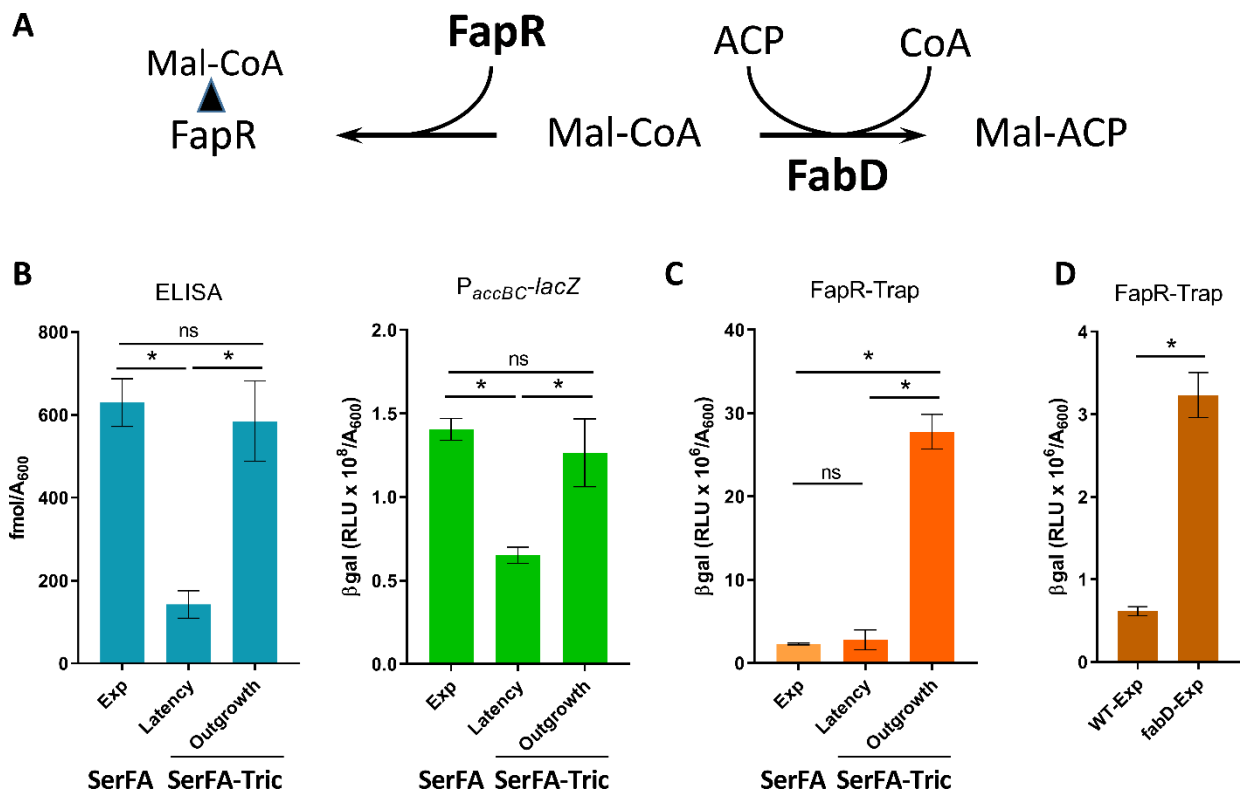

Fig. 3. Anti-FASII treatment leads to transient *acc* repression and shifts in malonyl-CoA distribution. A. The diagram illustrates two known malonyl-CoA interactants, FapR and FabD. FapR is a repressor of FASII and phospholipid synthesis. Malonyl-CoA binds FapR (left), which reverses FapR repressor activity. FabD uses malonyl-CoA to produce malonyl-ACP, the FASII precursor (right). **B.** Assessment of malonyl-CoA production by ELISA and P_{accBC}-*lacZ*. Left panel: Sandwich ELISA assay was used to measure total malonyl-CoA (Materials and Methods). Right panel: P_{accBC}-*lacZ* reporter activity. **C.** Assessment of FapR-bound malonyl-CoA. FASII-antibiotic-adapted *S. aureus* display altered malonyl-CoA distribution (**see A**). Newman strain and derivatives were grown in non-selective (SerFA) and anti-FASII (SerFA-Tric) media. β-gal activities were measured in SerFA at A_{600} = ~2.0 (exponential growth: Exp), and in SerFA-Tric during latency after 3 h growth A_{600} = ~0.3 (Latency) and upon adaptive exponential outgrowth A_{600} = ~2 (Outgrowth). **D.** Assessment of FapR-bound malonyl-CoA in a *fabD* mutant using FapR-Trap. β-gal assays of Newman and *fabD* mutant (CondT^R-17, a point mutant (4) carrying FapR-Trap were performed in SerFA after 3 h growth with A_{600} = ~1.0 (Exp). Measurements in **B** to **D** are mean ± standard deviation from triplicate independent experiments. *, $p \leq 0.05$, ns, not significant, using Mann Whitney.

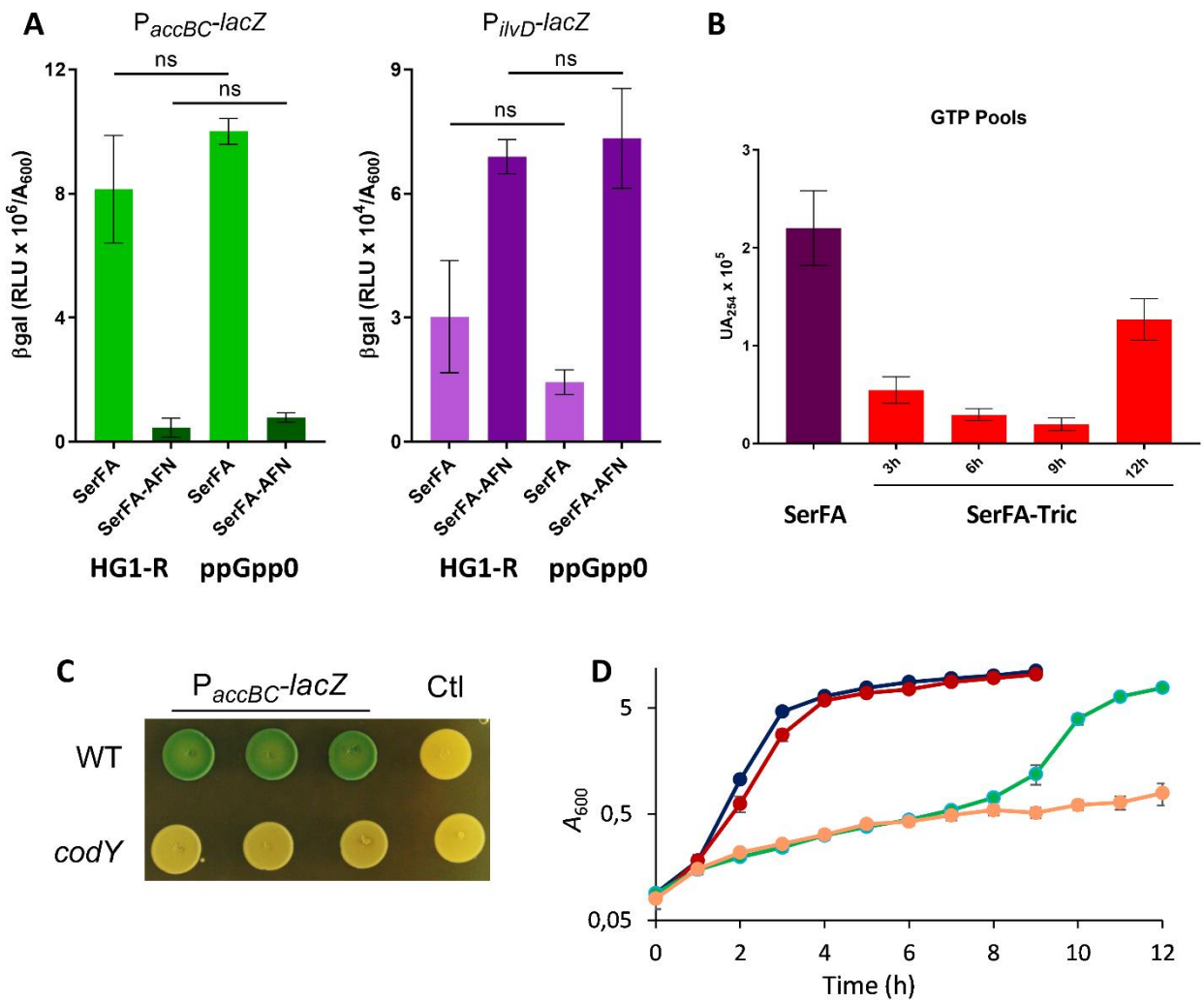

512

513 **Fig. 4. GTP is depleted during anti-FASII latency phase. A.** P_{accBC}-*lacZ* (left) and P_{ilvD}-*lacZ* (right)
514 sensor responses to anti-FASII latency were compared in *S. aureus* HG1-R and the (p)ppGpp null
515 isogenic strain as indicated. β-gal activities were measured after 3h incubation in SerFA and in
516 medium containing the anti-FASII AFN-1252. Data presented are mean ± standard deviation from
517 three biological replicates. P-values were determined pairwise by Mann Whitney; ns, not
518 significant. **B.** Newman strain GTP levels were assessed at different growth times during anti-FASII
519 latency (3h, 6h, and 9h) and outgrowth (12h). Data presented are mean ± standard deviation from
520 duplicate independent experiments. **C.** P_{accBC}–*lacZ* expression is lower in a *codY* mutant. USA300 and
521 *codY* derivative contain plasmids expressing P_{accBC}–*lacZ* or the control plasmid (pTCV-lac; Ctl).
522 Exponential phase cultures issued from three independent colonies were adjusted to A_{600} = 0.1 and
523 5µl drops were plated on BHI plates containing erythromycin (5 µg/ml) and X-gal. Photographs
524 were taken after 20 h at 37°C and 24 h at 4°C. **D.** Growth of *S. aureus* USA300 and a confirmed *codY*

525 mutant of the Nebraska mutant collection was compared in non-selective (SerFA) and SerFA-Tric
526 conditions in four independent replicates. WT in SerFA, black; *codY* in SerFA, red; WT in SerFA-Tric,
527 green; *codY* in SerFA-Tric, orange. Mean and standard deviation are shown for each time point.

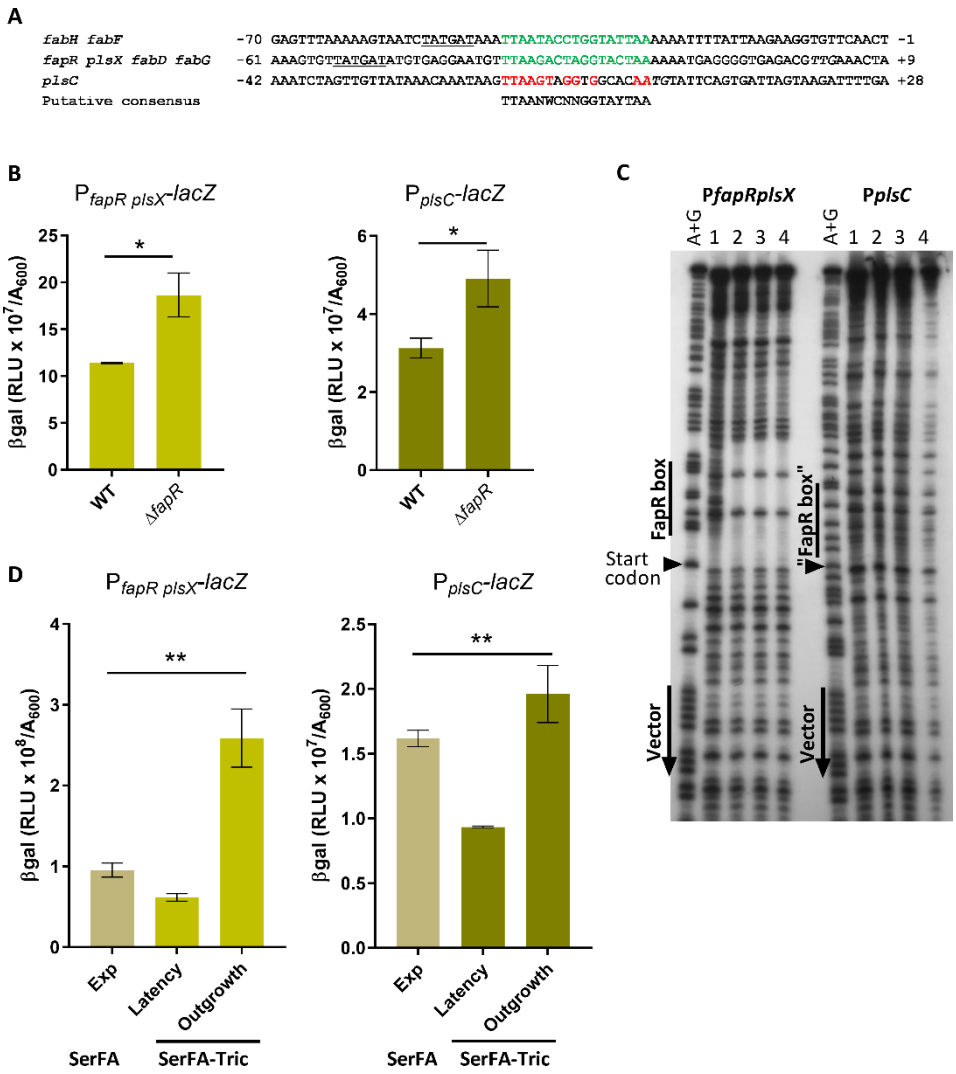

528

529 **Fig. 5. FapR binds the *plsX* but not the *plsC* promoter region, but affects expression of both genes.**
530 **A.** Sequence alignment of FapR binding sites in *S. aureus* as published (based on (13)). Positions
531 correspond to the predicted start codon of the first Orf in each operon. Confirmed 17 bp FapR
532 binding sequences are in green. The presumed conserved FapR binding nucleotides upstream of the
533 *plsC* start site are in red. In the consensus sequence below the alignment: N, any nucleotide; W, A
534 or T; Y, T or C. Putative -10 RNA polymerase binding sites are underlined (13). The PlsC ATG and
535 FapR TTG start sites are in italics. **B**. Expression of $P_{fapR\ plsX}$-*lacZ* and P_{plsC}-*lacZ* fusions is upregulated
536 in the Δ*fapR* strain. Strains were grown to A_{600} = ~1.5 in SerFA medium prior to β-gal
537 determinations. Data presented are mean ± standard deviation from three biological replicates. *, p
538 ≤ 0.05, ns, not significant, using Mann Whitney. **C.** DNase I footprinting assay of the *PfapRplsX* and
539 P*plsC* promoter regions with FapR. Radiolabeled PCR fragments corresponding to P*plsX* and P*plsC*
540 were used as DNA targets. Various amounts of FapR (lane 1: 0; lane 2: 1.2 nmol; lane 3: 6 nmol; and

541 lane 4: 12 nmol) were incubated with 0.2 pmol DNA before DNase 1 digestion. Lane A+G: Maxam
542 and Gilbert reaction of the labeled strand. Positions of vector and "FapR box" sequences are
543 indicated by vertical lines, PlsX and PlsC start codons are indicated by black arrows. **D.** Expression of
544 $P_{fapR\ plsX}$-*lacZ* and P_{plsC}-*lacZ* fusions in *S. aureus* Newman during growth in non-selective (SerFA) and
545 anti-FASII (SerFA-Tric) media. β-gal are shown for samples processed in SerFA at OD_{600} = ~2.0
546 (exponential phase, Exp), and in SerFA-Tric after 3h in latency (OD_{600} = ~0.3) and upon adaptation
547 outgrowth at 17 h (OD_{600} = ~2.0; Outgrowth). Mean and standard deviation are shown for three
548 independent experiments. P-values were determined by Kruskal Wallis; $p \leq 0.005$ is indicated by **;
549 ns, not significant.

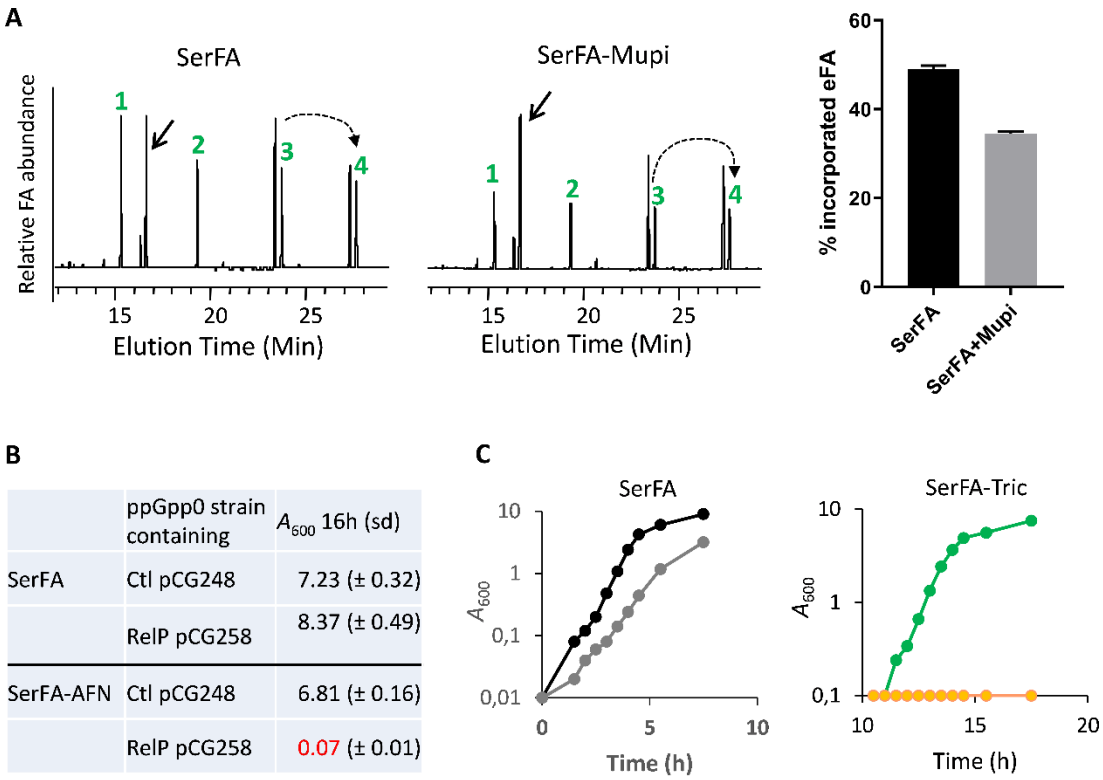

	ppGpp0 strain containing	A_{600} 16h (sd)
SerFA	Ctl pCG248	7.23 (± 0.32)
	RelP pCG258	8.37 (± 0.49)
SerFA-AFN	Ctl pCG248	6.81 (± 0.16)
	RelP pCG258	0.07 (± 0.01)

550

551 **Fig. 6. Subinhibitory mupirocin inhibits *S. aureus* eFA incorporation in membrane phospholipids**
552 **and synergizes with anti-FASII to inhibit adaptation. A.** Left, Fatty acid profiles of *S. aureus*
553 Newman grown in SerFA and SerFA+mupirocin (mupi). Samples were processed after 3 h growth.
554 Black arrow, position of the main endogenous fatty acid *ai*15:0. eFA are: 1- C14:0; 2- C16:0; 3-
555 C18:1; 4- C20:1 (elongation of C18:1). Dashed arrow, elongation of C18:1 (n+2). Right, percent eFA
556 of Newman grown in SerFA without and with Mupi, derived from integration of two fatty acid
557 profiles from two independent experiments. **B.** Control plasmid pCG248 and aTc-inducible *relP*-
558 expressing plasmid pCG258 (26) were established in the ppGpp0 (null) strain. Strains were grown in
559 SerFA and SerFA-AFN for 16h in the absence of inducer. Anti-FASII adaptation is inhibited in the
560 (p)ppGpp-expressing strain. **C.** Left, *S. aureus* Newman was grown in SerFA (black) and SerFA+mupi
561 (grey), or right, in SerFA-Tric (green) and SerFA-Tric+mupi (orange). Growth was monitored by A_{600}.
562 Growth curves at right are shown starting at 10 h. Mupi was used at 0.05 µg/ml. Results are
563 representative of three independent experiments.

564

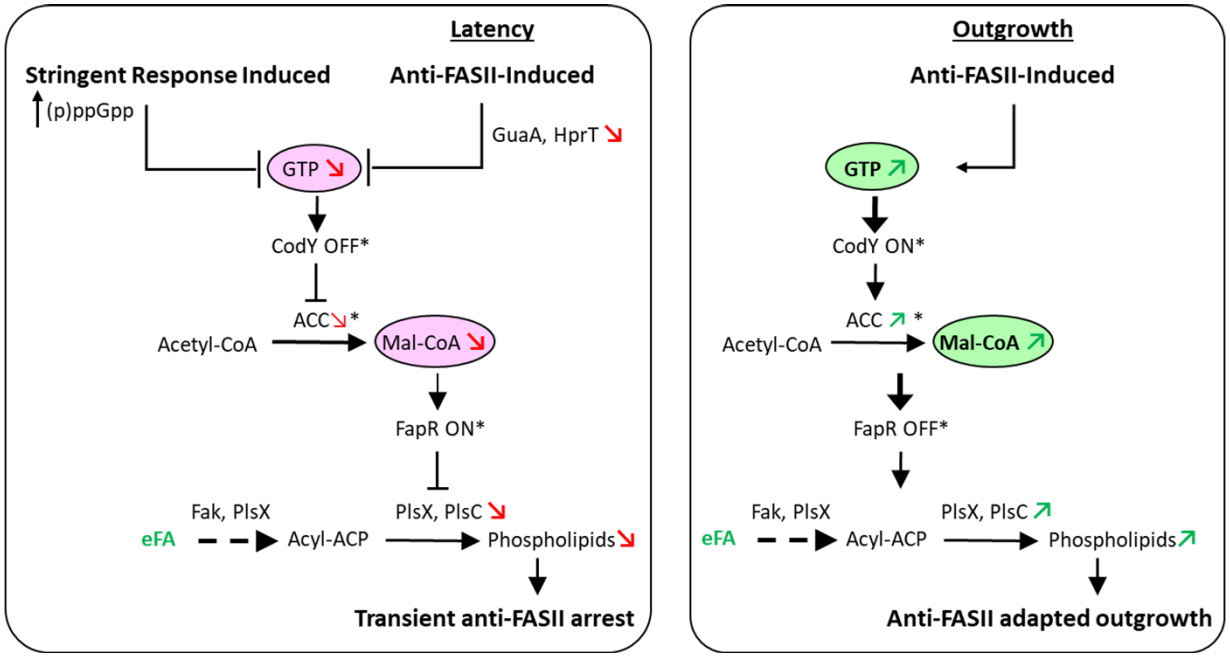

Fig. 7. Model for intersecting control of stringent response and FASII inhibition in *S. aureus*. Left: Stringent response induction leads to GTP depletion, which in turn modulates gene expression to prepare for starvation (20, 31). We showed that inhibition of FASII also leads to GTP depletion, pointing to an intersecting link between these pathways. Both conditions activate stringent response sensors (P_{ilvD}-*lacZ*, P_{oppB}-*lacZ*, and P_{cshA}-*lacZ*) and lower malonyl-CoA (mal-CoA) pools, such that FapR (for which mal-CoA acts as anti-repressor) exerts repression (13). As a consequence, genes under FapR control, including PlsX and PlsC, remain repressed, blocking phospholipid synthesis. Both stringent response induction and FASII inhibition during the latency phase lead to membrane synthesis arrest. **Right:** Upon FASII adaptation, GTP levels are restored. *accBC* expression is restored to normal, and mal-CoA levels are increased, leading to FapR derepression. In consequence, PlsX and PlsC are both increased, such that phospholipid synthesis resumes. Red and green arrows and circled metabolites correspond to functions analyzed in this study.

581 **Supplementary information titles and legends**

582 **Supplementary Fig. S1. *S. aureus* bypasses FASII inhibition by exogenous fatty acid (eFA)**
583 **incorporation in membrane phospholipids. A.** Model for anti-FASII adaptation. FASII and FASII
584 bypass are schematized as characterized; functions whose expression is controlled by FapR
585 repressor are underlined (1-4). Malonyl-CoA reverses FapR repression (5). eFA phosphorylation by
586 Fak (fatty acid kinase) (6) provides an intermediate that may either be incorporated in position 1 of
587 the glycerol-3-phosphate backbone *via* PlsY, or act as a substrate for PlsX to then be incorporated in
588 position 2 via PlsC. In the absence of serum, FabD (malonyl-CoA:ACP transacylase) mutations
589 promote anti-FASII adaptation (2). In contrast, serum favors FASII antibiotic adaptation without
590 FASII mutations (7). **B.** Example of fatty acid profiles of *S. aureus* Newman. Left, BHI grown cells;
591 right, cells grown overnight in SerFA-Tric. Cultures started at A_{600} = 0.01 were harvested at A_{600} = 1.
592 Arrow indicates *anteiso* 15 (*ai*15), the major fatty acid synthesized by *S. aureus*. eFA: 1, C14:0; 2,
593 C16:0; 3, 18:1. Profiles are representative of three independent experiments. FA, fatty acids; FA-
594 ACP, fatty acyl-ACP; FA-PO_4, acyl-phosphate; grey, inhibited pathway. FabD*, mutated or inhibited
595 enzyme.

596 **Supplementary Fig. S2. Responses of P_{ilvD}-*lacZ*, P_{cshA}-*lacZ*, and P_{accBC}-*lacZ* to mupirocin depend on**
597 **the presence of (p)ppGpp.** HG1-R is an HG001 derivative repaired for a *fakB1* defect common to
598 the 8325 lineage (1). ppGpp0 is the HGR-1 strain devoid of the three synthase genes *rsh*, *relP*, and
599 *relQ* (2). The indicated strains were plated (1 ml of A_{600} = 0.1) on BHI medium containing 100 µg/ml
600 X-gal and 5 µg/ml erythromycin and allowed to dry. Mupirocin (75, 37.5, 18.3, and 9.1 ng in rows
601 starting from upper left) was deposited in 3 µl drops. **A**. Expression of P_{ilvD}-*lacZ* is induced by
602 mupirocin (Fig. 1A), seen as a blue ring in HG1-R, which is absent in the ppGpp0 strain. **B**. P_{cshA}-*lacZ*
603 is repressed by mupirocin (Fig. 1A), seen as a non-blue growth ring, which is quasi-absent in the
604 ppGpp0 strain. **C.** The P_{accBC}-*lacZ* sensor behaves like P_{cshA}-*lacZ*, indicating that production of
605 malonyl-CoA by ACC is repressed by the stringent response. Plates were photographed after 24 h at
606 37°C and 24 h at 4°C. Dark zones indicate growth inhibition by mupirocin. The ppGpp0 strain is
607 more sensitive to mupirocin than the isogenic parent. Experiments were performed three times
608 giving comparable results.

609 **Supplementary Fig. S3. FapR-Trap, a malonyl-CoA sensor based on FapR operon *lacZ* fusion.**

610 **A.** Schematic design of FapR-Trap (pJJ004, Table S1). Malonyl-CoA (red diamond) binds FapR
611 (pacman) leading to its release from the FapR binding site (bar code) and expression of *lacZ* (blue)
612 to produce β-galactosidase. The 17 bp FapR consensus binding site used in the construction is
613 shown (based on (1)); converging arrows indicate the 8 bp inverted repeat. **B.** Validation of the
614 FapR-Trap as sensor. β-gal assays were performed with RN4220 and its Δ*fapR* derivative
615 $RN4220_{\Delta fapR}$ (1) carrying FapR-Trap after 3 h growth in SerFA (left). FapR-Trap expression was also
616 compared in exponential (Exp) and stationary phase (Stat) of the Newman strain (right). Data
617 presented are mean ± standard deviation from triplicate independent experiments. *, $p \leq 0.05$
618 using Mann Whitney.

619 **Table S1. Strains used in this study.**

620 **Table S2. Plasmids and constructions.**

621 **Table S3. Total and proportion of FapR-bound malonyl-CoA depends on growth condition.**

622 **Table S4. Responses of FapR regulon genes and known stringent response induced genes to**
623 **mupirocin.**

624 **Table S5. Subinhibitory mupirocin treatment synergizes with AFN-1252 to inhibits MRSA USA300**
625 **growth.**

626 **Table S6. Primers.**

627 **References:**

628

629 1. Uchil RR, Kohli GS, Katekhaye VM, Swami OC. 2014. Strategies to combat antimicrobial resistance. J
630 Clin Diagn Res 8:ME01-4.

631 2. Lu H, Tonge PJ. 2008. Inhibitors of FabI, an enzyme drug target in the bacterial fatty acid biosynthesis
632 pathway. Acc Chem Res 41:11-20.

633 3. Brinster S, Lamberet G, Staels B, Trieu-Cuot P, Gruss A, Poyart C. 2009. Type II fatty acid synthesis is
634 not a suitable antibiotic target for Gram-positive pathogens. Nature 458:83-6.

635 4. Morvan C, Halpern D, Kenanian G, Hays C, Anba-Mondoloni J, Brinster S, Kennedy S, Trieu-Cuot P,
636 Poyart C, Lamberet G, Gloux K, Gruss A. 2016. Environmental fatty acids enable emergence of
637 infectious *Staphylococcus aureus* resistant to FASII-targeted antimicrobials. Nat Commun 7:12944.

638 5. Kenanian G, Morvan C, Weckel A, Pathania A, Anba-Mondoloni J, Halpern D, Gaillard M, Solgadi A,
639 Dupont L, Henry C, Poyart C, Fouet A, Lamberet G, Gloux K, Gruss A. 2019. Permissive Fatty Acid
640 Incorporation Promotes Staphylococcal Adaptation to FASII Antibiotics in Host Environments. Cell
641 Rep 29:3974-3982 e4.

642 6. Wang J, Soisson SM, Young K, Shoop W, Kodali S, Galgoci A, Painter R, Parthasarathy G, Tang YS,
643 Cummings R, Ha S, Dorso K, Motyl M, Jayasuriya H, Ondeyka J, Herath K, Zhang C, Hernandez L,
644 Allocco J, Basilio A, Tormo JR, Genilloud O, Vicente F, Pelaez F, Colwell L, Lee SH, Michael B, Felcetto
645 T, Gill C, Silver LL, Hermes JD, Bartizal K, Barrett J, Schmatz D, Becker JW, Cully D, Singh SB. 2006.
646 Platensimycin is a selective FabF inhibitor with potent antibiotic properties. Nature 441:358-61.

647 7. Banevicius MA, Kaplan N, Hafkin B, Nicolau DP. 2013. Pharmacokinetics, pharmacodynamics and
648 efficacy of novel FabI inhibitor AFN-1252 against MSSA and MRSA in the murine thigh infection
649 model. J Chemother 25:26-31.

650 8. Escaich S, Prouvensier L, Saccomani M, Durant L, Oxoby M, Gerusz V, Moreau F, Vongsouthi V,
651 Maher K, Morrissey I, Soulama-Mouze C. 2011. The MUT056399 inhibitor of FabI is a new
652 antistaphylococcal compound. Antimicrob Agents Chemother 55:4692-7.

653 9. Feng Z, Chakraborty D, Dewell SB, Reddy BV, Brady SF. 2012. Environmental DNA-encoded
654 antibiotics fasamycins A and B inhibit FabF in type II fatty acid biosynthesis. J Am Chem Soc
655 134:2981-7.

656 10. Pishchany G, Mevers E, Ndousse-Fetter S, Horvath DJ, Jr., Paludo CR, Silva-Junior EA, Koren S, Skaar
657 EP, Clardy J, Kolter R. 2018. Amycomicin is a potent and specific antibiotic discovered with a targeted
658 interaction screen. Proc Natl Acad Sci U S A 115:10124-10129.

659 11. Parsons JB, Frank MW, Subramanian C, Saenkham P, Rock CO. 2011. Metabolic basis for the
660 differential susceptibility of Gram-positive pathogens to fatty acid synthesis inhibitors. Proc Natl
661 Acad Sci U S A 108:15378-83.

662 12. Gloux K, Guillemet M, Soler C, Morvan C, Halpern D, Pourcel C, Vu Thien H, Lamberet G, Gruss A.
663 2017. Clinical Relevance of Type II Fatty Acid Synthesis Bypass in *Staphylococcus aureus*. Antimicrob
664 Agents Chemother 61.

665 13. Albanesi D, Reh G, Guerin ME, Schaeffer F, Debarbouille M, Buschiazzo A, Schujman GE, de Mendoza
666 D, Alzari PM. 2013. Structural basis for feed-forward transcriptional regulation of membrane lipid
667 homeostasis in *Staphylococcus aureus*. PLoS Pathog 9:e1003108.

668 14. Albanesi D, de Mendoza D. 2016. FapR: From Control of Membrane Lipid Homeostasis to a
669 Biotechnological Tool. Front Mol Biosci 3:64.

670 15. Ruch FE, Vagelos PR. 1973. The isolation and general properties of *Escherichia coli* malonyl
671 coenzyme A-acyl carrier protein transacylase. J Biol Chem 248:8086-94.

672 16. Nazir A, Harinarayanan R. 2016. (p)ppGpp and the bacterial cell cycle. J Biosci 41:277-82.

673 17. Potrykus K, Cashel M. 2008. (p)ppGpp: still magical? Annu Rev Microbiol 62:35-51.

674 18. My L, Rekoske B, Lemke JJ, Viala JP, Gourse RL, Bouveret E. 2013. Transcription of the *Escherichia coli*
675 fatty acid synthesis operon *fabHDG* is directly activated by FadR and inhibited by ppGpp. J Bacteriol
676 195:3784-95.

677 19. Janssen HJ, Steinbuchel A. 2014. Fatty acid synthesis in *Escherichia coli* and its applications towards
678 the production of fatty acid based biofuels. Biotechnol Biofuels 7:7.

679 20. Pulschen AA, Sastre DE, Machinandiarena F, Crotta Asis A, Albanesi D, de Mendoza D, Gueiros-Filho
680 FJ. 2017. The stringent response plays a key role in Bacillus subtilis survival of fatty acid starvation.
681 Mol Microbiol 103:698-712.

682 21. Vadia S, Tse JL, Lucena R, Yang Z, Kellogg DR, Wang JD, Levin PA. 2017. Fatty Acid Availability Sets
683 Cell Envelope Capacity and Dictates Microbial Cell Size. Curr Biol 27:1757-1767 e5.

684 22. Greenwood RC, Gentry DR. 2002. The effect of antibiotic treatment on the intracellular nucleotide
685 pools of *Staphylococcus aureus*. FEMS Microbiol Lett 208:203-6.

686 23. Rhee HW, Lee CR, Cho SH, Song MR, Cashel M, Choy HE, Seok YJ, Hong JI. 2008. Selective fluorescent
687 chemosensor for the bacterial alarmone (p)ppGpp. J Am Chem Soc 130:784-5.

688 24. Geiger T, Francois P, Liebeke M, Fraunholz M, Goerke C, Krismer B, Schrenzel J, Lalk M, Wolz C. 2012.
689 The stringent response of *Staphylococcus aureus* and its impact on survival after phagocytosis
690 through the induction of intracellular PSMs expression. PLoS Pathog 8:e1003016.

691 25. Herbert S, Ziebandt AK, Ohlsen K, Schafer T, Hecker M, Albrecht D, Novick R, Gotz F. 2010. Repair of
692 global regulators in *Staphylococcus aureus* 8325 and comparative analysis with other clinical isolates.
693 Infect Immun 78:2877-89.

694 26. Geiger T, Kastle B, Gratani FL, Goerke C, Wolz C. 2014. Two small (p)ppGpp synthases in
695 *Staphylococcus aureus* mediate tolerance against cell envelope stress conditions. J Bacteriol
696 196:894-902.

697 27. Parsons JB, Broussard TC, Bose JL, Rosch JW, Jackson P, Subramanian C, Rock CO. 2014. Identification
698 of a two-component fatty acid kinase responsible for host fatty acid incorporation by *Staphylococcus*
699 *aureus*. Proc Natl Acad Sci U S A 111:10532-7.

700 28. Parsons JB, Frank MW, Rosch JW, Rock CO. 2013. *Staphylococcus aureus* fatty acid auxotrophs do
701 not proliferate in mice. Antimicrob Agents Chemother 57:5729-32.

702 29. Polakis SE, Guchhait RB, Lane MD. 1973. Stringent control of fatty acid synthesis in *Escherichia coli*.
703 Possible regulation of acetyl coenzyme A carboxylase by ppGpp. J Biol Chem 248:7957-66.

704 30. Kriel A, Bittner AN, Kim SH, Liu K, Tehranchi AK, Zou WY, Rendon S, Chen R, Tu BP, Wang JD. 2012.
705 Direct regulation of GTP homeostasis by (p)ppGpp: a critical component of viability and stress
706 resistance. Mol Cell 48:231-41.

707 31. Geiger T, Wolz C. 2014. Intersection of the stringent response and the CodY regulon in low GC Gram-
708 positive bacteria. Int J Med Microbiol 304:150-5.

709 32. Rajamuthiah R, Jayamani E, Conery AL, Fuchs BB, Kim W, Johnston T, Vilcinskas A, Ausubel FM,
710 Mylonakis E. 2015. A Defensin from the Model Beetle Tribolium castaneum Acts Synergistically with
711 Telavancin and Daptomycin against Multidrug Resistant *Staphylococcus aureus*. PLoS One
712 10:e0128576.

713 33. Gao W, Chua K, Davies JK, Newton HJ, Seemann T, Harrison PF, Holmes NE, Rhee HW, Hong JI,
714 Hartland EL, Stinear TP, Howden BP. 2010. Two novel point mutations in clinical *Staphylococcus*
715 *aureus* reduce linezolid susceptibility and switch on the stringent response to promote persistent
716 infection. PLoS Pathog 6:e1000944.

717 34. Kizer L, Pitera DJ, Pfleger BF, Keasling JD. 2008. Application of functional genomics to pathway
718 optimization for increased isoprenoid production. Appl Environ Microbiol 74:3229-41.

719 35. Machinandiarena F, Nakamatsu L, Schujman GE, de Mendoza D, Albanesi D. 2020. Revisiting the
720 coupling of fatty acid to phospholipid synthesis in bacteria with FapR regulation. Mol Microbiol
721 doi:10.1111/mmi.14574.

722 36. Kumari R, Saxena R, Tiwari S, Tripathi DK, Srivastava KK. 2013. Rv3080c regulates the rate of
723 inhibition of mycobacteria by isoniazid through FabD. Mol Cell Biochem 374:149-55.

724 37. Johnson AO, Gonzalez-Villanueva M, Wong L, Steinbuchel A, Tee KL, Xu P, Wong TS. 2017. Design
725 and application of genetically-encoded malonyl-CoA biosensors for metabolic engineering of
726 microbial cell factories. Metab Eng 44:253-264.

727 38. Goldmann O, Cern A, Musken M, Rohde M, Weiss W, Barenholz Y, Medina E. 2019. Liposomal
728 mupirocin holds promise for systemic treatment of invasive *Staphylococcus aureus* infections. J
729 Control Release 316:292-301.

730 39. Poyart C, Trieu-Cuot P. 1997. A broad-host-range mobilizable shuttle vector for the construction of
731 transcriptional fusions to beta-galactosidase in gram-positive bacteria. FEMS Microbiol Lett 156:193-
732 8.

733 40. Reiss S, Pane-Farre J, Fuchs S, Francois P, Liebeke M, Schrenzel J, Lindequist U, Lalk M, Wolz C,
734 Hecker M, Engelmann S. 2012. Global analysis of the *Staphylococcus aureus* response to mupirocin.
735 Antimicrob Agents Chemother 56:787-804.

736 41. Fernandez C, Gaspar C, Torrellas A, Vindel A, Saez-Nieto JA, Cruzet F, Aguilar L. 1995. A double-blind,
737 randomized, placebo-controlled clinical trial to evaluate the safety and efficacy of mupirocin calcium
738 ointment for eliminating nasal carriage of *Staphylococcus aureus* among hospital personnel. J
739 Antimicrob Chemother 35:399-408.

740 42. McMurry LM, Oethinger M, Levy SB. 1998. Triclosan targets lipid synthesis. Nature 394:531-2.

741 43. Mistou MY, Dramsi S, Brega S, Poyart C, Trieu-Cuot P. 2009. Molecular dissection of the secA2 locus
742 of group B Streptococcus reveals that glycosylation of the Srr1 LPXTG protein is required for full
743 virulence. J Bacteriol 191:4195-206.

744 44. Biswas I, Gruss A, Ehrlich SD, Maguin E. 1993. High-efficiency gene inactivation and replacement
745 system for gram-positive bacteria. J Bacteriol 175:3628-35.

746 45. Kraemer GRK, Iandolo JJ. 1990. High-frequency transformation of *Staphylococcus aureus* by
747 electroporation. Curr Microbiol 21:373.

748 46. Anderson KL, Roberts C, Disz T, Vonstein V, Hwang K, Overbeek R, Olson PD, Projan SJ, Dunman PM.
749 2006. Characterization of the *Staphylococcus aureus* heat shock, cold shock, stringent, and SOS
750 responses and their effects on log-phase mRNA turnover. J Bacteriol 188:6739-56.

751 47. Ellis JM, Wolfgang MJ. 2012. A genetically encoded metabolite sensor for malonyl-CoA. Chem Biol
752 19:1333-9.

753 48. Lechardeur D, Cesselin B, Liebl U, Vos MH, Fernandez A, Brun C, Gruss A, Gaudu P. 2012. Discovery
754 of intracellular heme-binding protein HrtR, which controls heme efflux by the conserved HrtB-HrtA
755 transporter in *Lactococcus lactis*. J Biol Chem 287:4752-8.

756 49. Munier H, Gilles AM, Glaser P, Krin E, Danchin A, Sarfati R, Barzu O. 1991. Isolation and
757 characterization of catalytic and calmodulin-binding domains of *Bordetella pertussis* adenylate
758 cyclase. Eur J Biochem 196:469-74.

759 50. Derre I, Rapoport G, Msadek T. 1999. CtsR, a novel regulator of stress and heat shock response,
760 controls clp and molecular chaperone gene expression in gram-positive bacteria. Mol Microbiol
761 31:117-31.

762

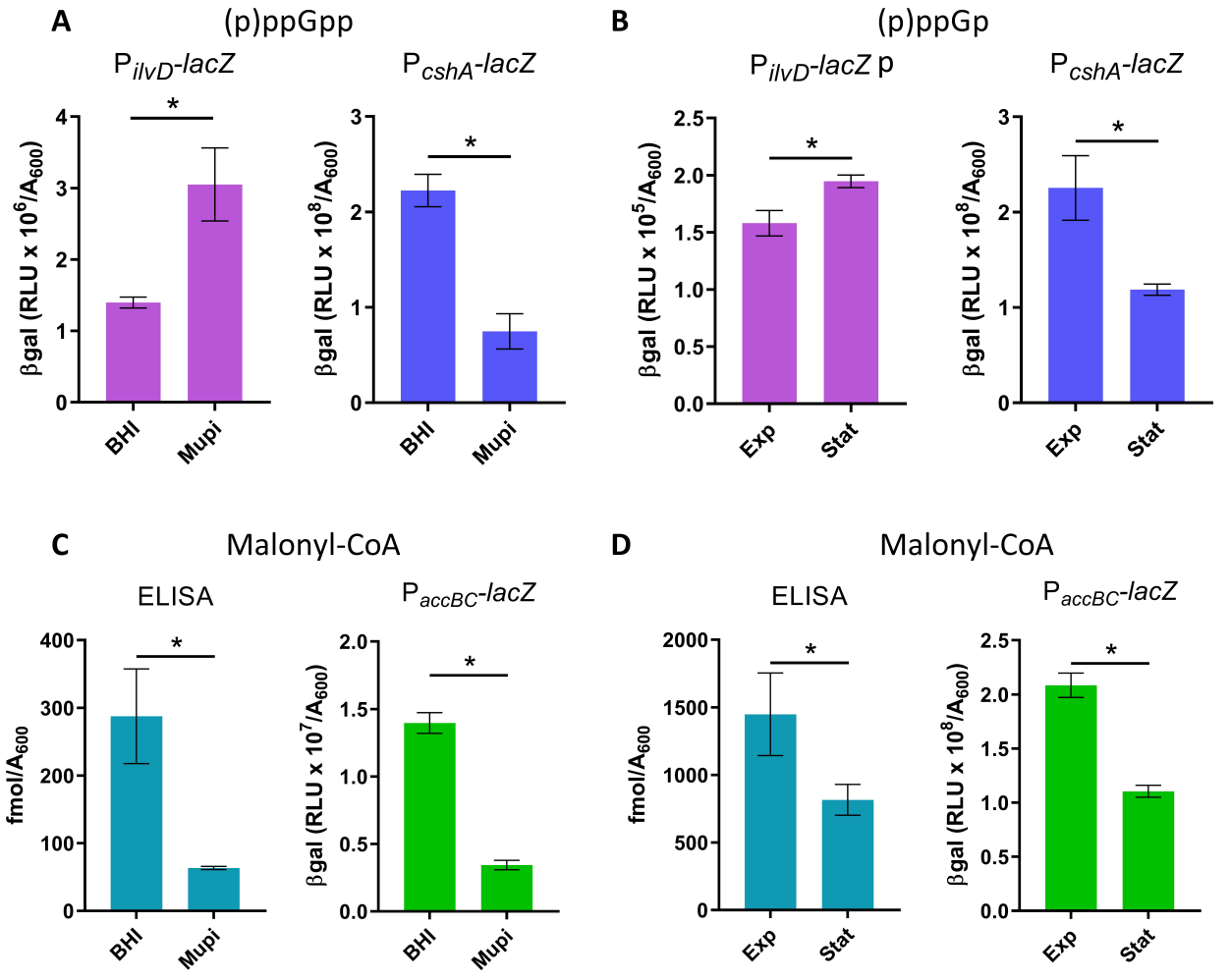
A
(p)ppGpp
PilvD-lacZ
βgal (RLU x 10^6/A600)
BHI
Mupi
PcshA-lacZ
βgal (RLU x 10^8/A600)
B
(p)ppGp
PilvD-lacZ p
βgal (RLU x 10^5/A600)
Exp
Stat
PcshA-lacZ
βgal (RLU x 10^8/A600)
C
Malonyl-CoA
ELISA
fmol/A600
PaccBC-lacZ
βgal (RLU x 10^7/A600)
D
Malonyl-CoA
ELISA
fmol/A600
PaccBC-lacZ
βgal (RLU x 10^8/A600)

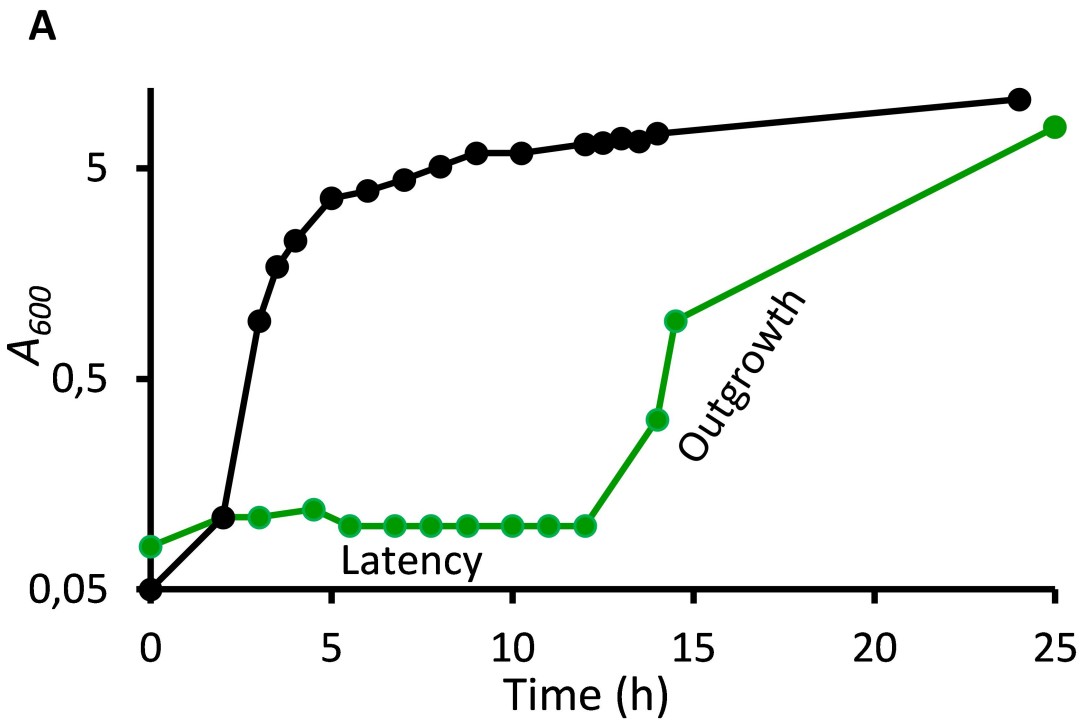
A
A_{600}
5
0,5
0,05
Latency
Outgrowth
0
5
10
15
20
25
Time (h)

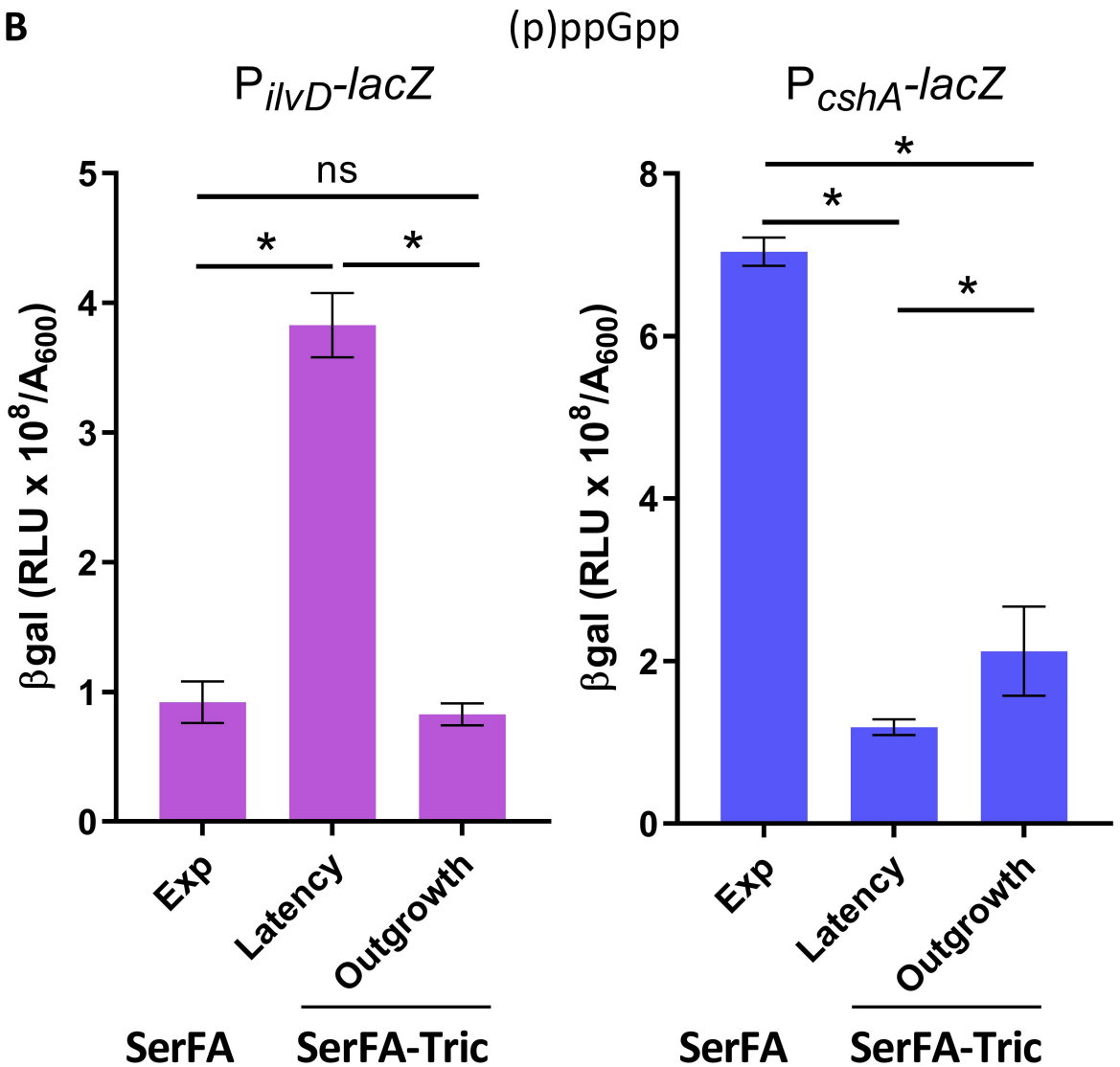
B
(p)ppGpp
P_{ilvD}-*lacZ*
P_{cshA}-*lacZ*
ns
*
βgal (RLU x $10^8/A_{600}$)
Exp
Latency
Outgrowth
SerFA
SerFA-Tric

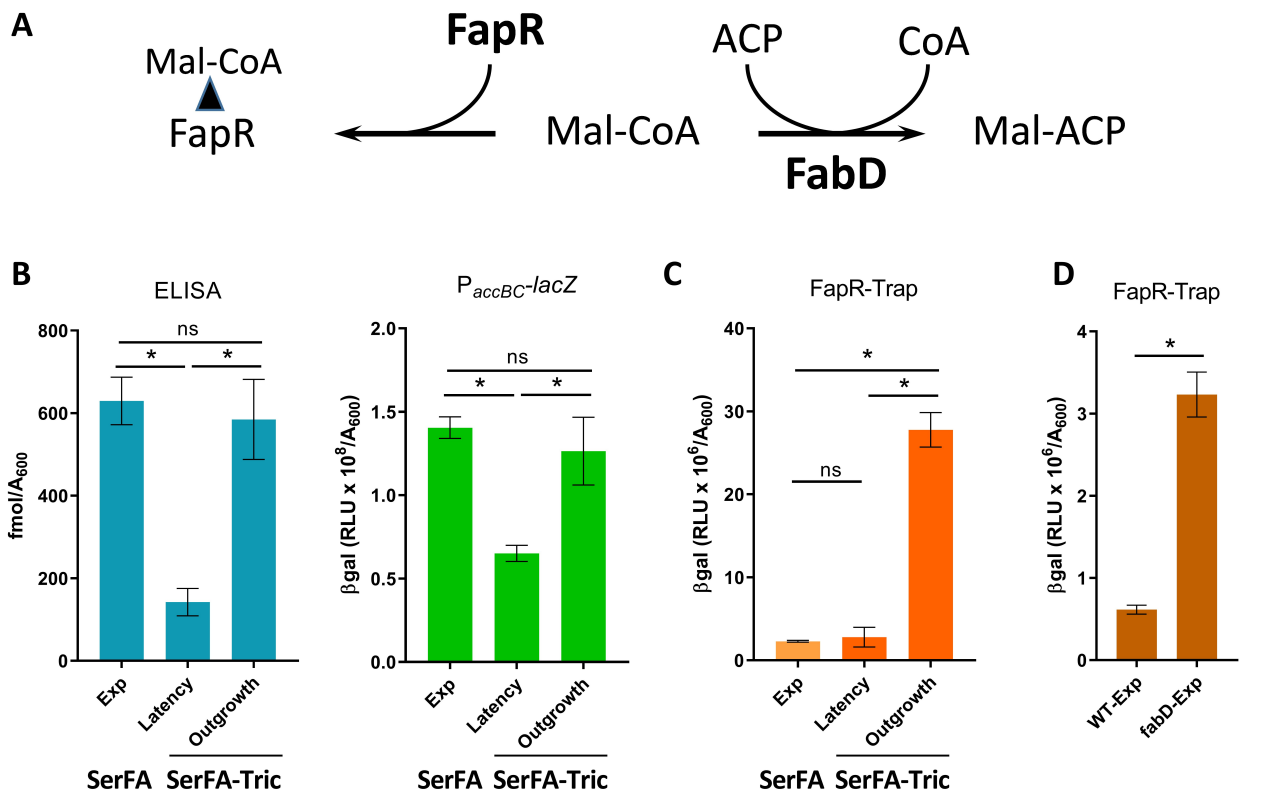
A
Mal-CoA
FapR
FapR
Mal-CoA
ACP
CoA
FabD
Mal-ACP
B
ELISA
fmol/A600
800
600
400
200
0
ns
*
*
Exp
Latency
Outgrowth
SerFA
SerFA-Tric
PaccBC-lacZ
βgal (RLU x 10^8/A600)
2.0
1.5
1.0
0.5
0.0
ns
*
*
Exp
Latency
Outgrowth
SerFA
SerFA-Tric
C
FapR-Trap
βgal (RLU x 10^6/A600)
40
30
20
10
0
*
*
ns
Exp
Latency
Outgrowth
SerFA
SerFA-Tric
D
FapR-Trap
βgal (RLU x 10^6/A600)
4
3
2
1
0
*
WT-Exp
fabD-Exp

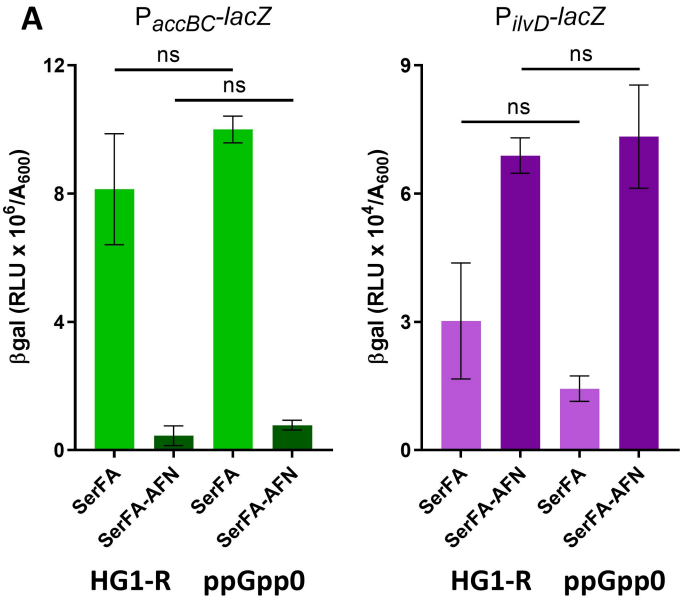
A
PaccBC-lacZ
PilvD-lacZ
ns
βgal (RLU x 10^6/A600)
βgal (RLU x 10^4/A600)
SerFA
SerFA-AFN
HG1-R
ppGpp0

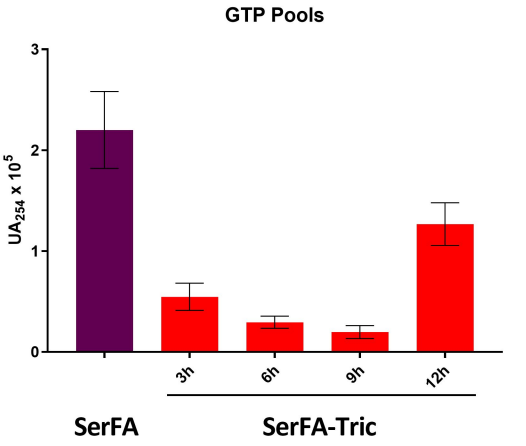
B
GTP Pools
UA254 x 10^5
3h
6h
9h
12h
SerFA
SerFA-Tric

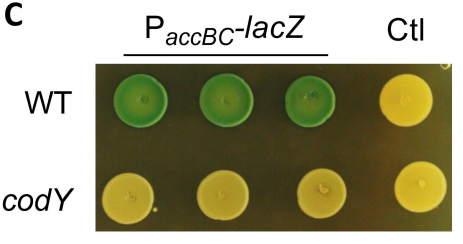
C
PaccBC-lacZ
Ctl
WT
codY

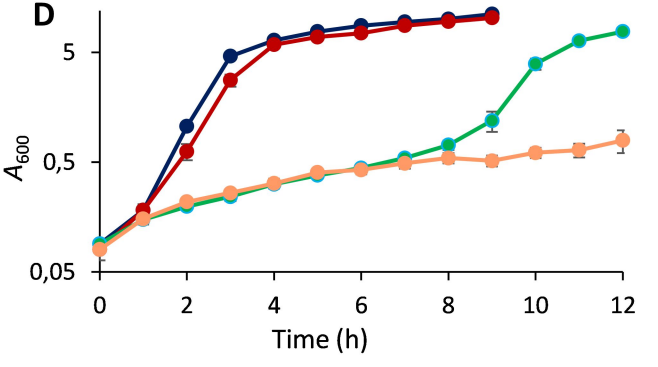
D
A600
Time (h)

A

```
fabH fabF          -70 GAGTTTAAAAAGTAATCTATGATAAATTAATACCTGGTATTAAAAAATTTTATTAAGAAGGTGTTCAACT -1
fapR plsX fabD fabG -61 AAAGTGTTATGATATGTGAGGAATGTTTAAGACTAGGTACTAAAAAATGAGGGGTGAGACGTTGAAACTA +9
plsC               -42 AAATCTAGTTGTTATAAACAAATAAGTTAAGTAGGTGGCACAATGTATTCAGTGATTAGTAAGATTTTGA +28
Putative consensus                                 TTAANWCNNGGTAYTAA
```

B

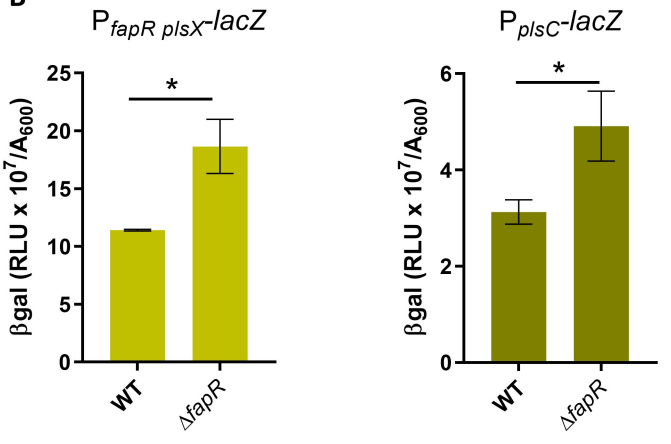

C

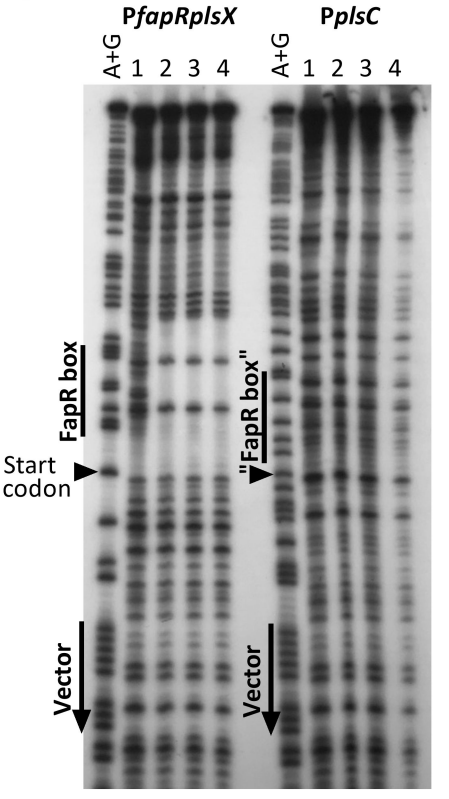

D

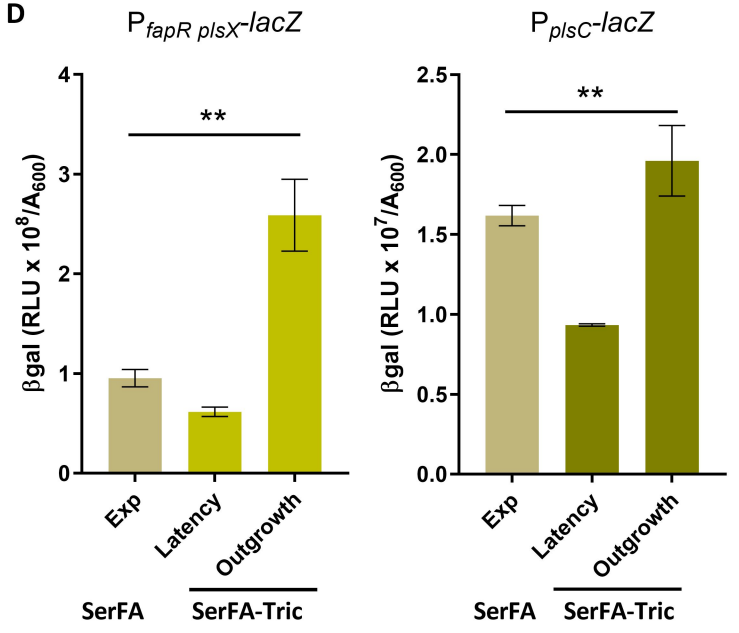

A

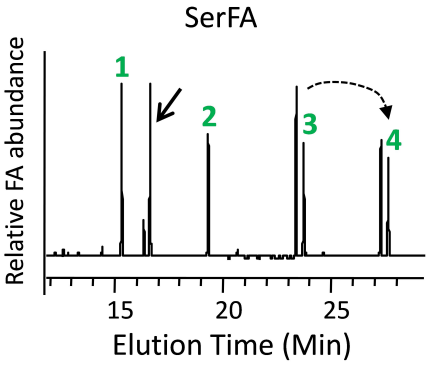

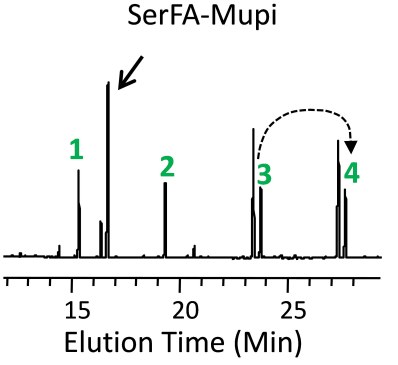

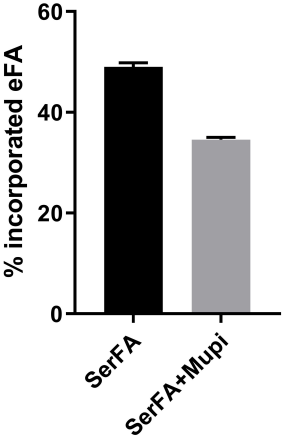

B

	ppGpp0 strain containing	A_{600} 16h (sd)
SerFA	Ctl pCG248	7.23 (± 0.32)
	RelP pCG258	8.37 (± 0.49)
SerFA-AFN	Ctl pCG248	6.81 (± 0.16)
	RelP pCG258	0.07 (± 0.01)

C

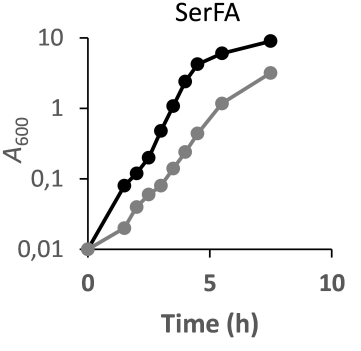

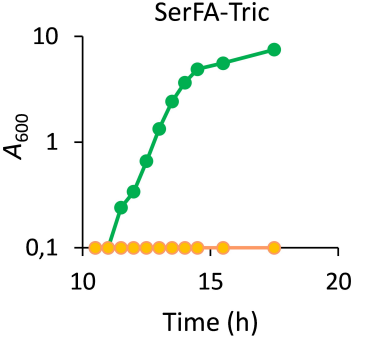

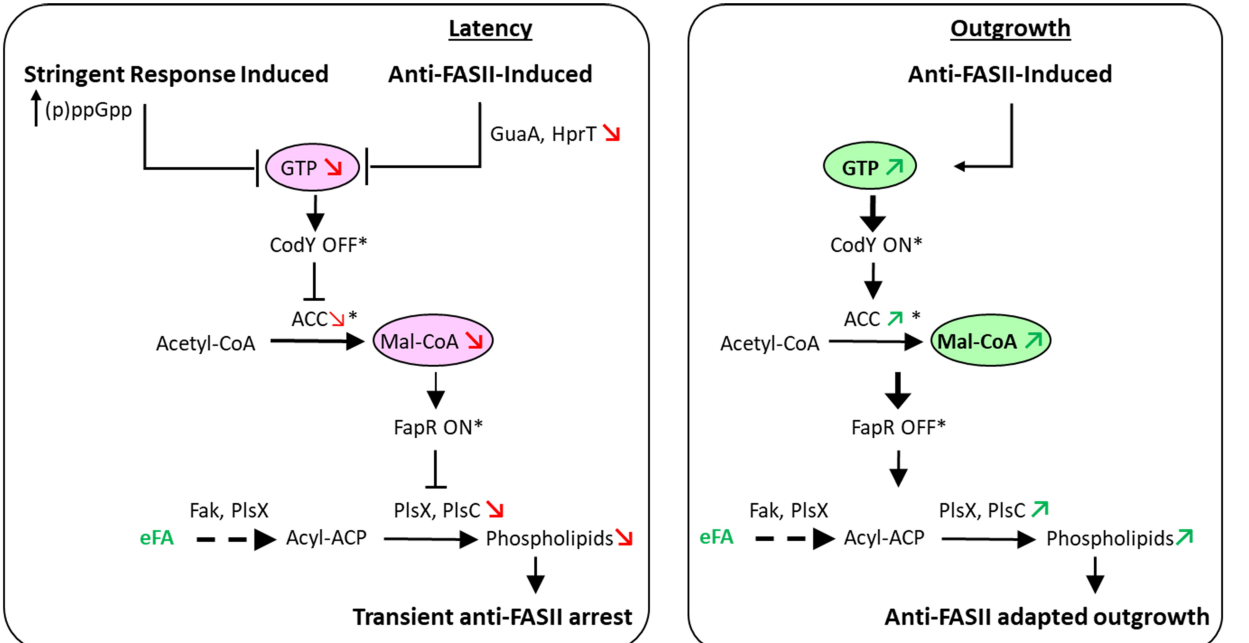
Latency
Stringent Response Induced
Anti-FASII-Induced
(p)ppGpp
GuaA, HprT
GTP
CodY OFF*
ACC *
Acetyl-CoA
Mal-CoA
FapR ON*
Fak, PlsX
PlsX, PlsC
eFA
Acyl-ACP
Phospholipids
Transient anti-FASII arrest
Outgrowth
Anti-FASII-Induced
GTP
CodY ON*
ACC *
Acetyl-CoA
Mal-CoA
FapR OFF*
Fak, PlsX
PlsX, PlsC
eFA
Acyl-ACP
Phospholipids
Anti-FASII adapted outgrowth